Contents

IFFS Malaysia Meeting 2026

Meeting Program

27-31 July 2026

Bangi Resort Hotel, Kuala Lumpur, Malaysia

Monday, 27 July 2026

Venue: Lobby, Bangi Resort Hotel

On-site Registration

Time	Program
14:00-17:00	On-site Registration and Conference Materials Collection

Tuesday, 28 July 2026

Venue: Melur Hall at Level 3, Bangi Resort Hotel

Time	Program	
09:00-09:25	Opening Ceremony	
Melur Hall at Level 3		
Session: Quantum Information, Optical Sensing and Optoelectronics Chair: Arup Neogi		
09:25-09:50	**A01:** Quantum Many-Body Sensors	**Abolfazl Bayat** University of Electronic Science and Technology of China, China
09:50-10:15	**A02:** Achieving Heisenberg Limit Under Noisy Conditions With Quantum Zeno Dynamics and Dynamical Decoupling	**Tan Kok Chuan Bobby** Institute of Fundamental and Frontier Sciences, University of Electronic Science and Technology of China, China
10:15-10:35	**Coffee Break**	
10:35-11:00	**A03:** High-Precision Computational Reconstruction Integrated Spectroscopy Technology	**Xue Tong** Tianfu Jiangxi Laboratory, China
11:00-11:25	**A04:** Nanoscale Energy Converters: Bridging Optoelectronics and Photothermal Applications	**Zhiming Wang** Tianfu Jiangxi Laboratory, China
11:25-11:50	**A05:** Research and Development of High-Efficiency Semiconductor Optoelectronic Functional Materials, Device Integration and First-Principles Studies	**Chengxin Zhou** Shimmer Center, Tianfu Jiangxi Laboratory, China
11:50-14:00	**Lunch Break**	

Tuesday, 28 July 2026

Venue: Melur Hall at Level 3, Bangi Resort Hotel

Melur Hall at Level 3		
Session: Photonic, Semiconductor and Functional Nanomaterials Chair: Zhiming Wang		
14:00-14:25	**A06:** Development of High-Performance Organic Near-Infrared Upconversion Devices for Optoelectronic Signal Coordination and Biomedical Applications	**Zeyu He** Shimmer Center, Tianfu Jiangxi Laboratory, China
14:25-14:50	**A07:** Controllable Preparation, Doping Modification, and Heterojunction Device Research of PbSe-Based Photodetection Materials	**Silu Peng** Shimmer Center, Tianfu Jiangxi Laboratory, China
14:50-15:15	**A08: CANCELED**	
14:50-15:35	**Coffee Break**	
15:35-16:00	**A09:** SERS for Detection and Biodetection	**Ramon A. Alvarez-Puebla** ICREA and Universitat Rovira i Virgili, Spain
16:00-16:25	**A10:** Low-Dimensional Materials: Synthesis, Characterization, Applications, and First-Principles Calculations	**Chang Fu Dee** Institute of Microengineering and Nanoelectronics, Universiti Kebangsaan Malaysia, Malaysia
16:25-16:50	**A11: CANCELED**	

Wednesday, 29 July 2026

Venue: Melur Hall at Level 3, Bangi Resort Hotel

Melur Hall at Level 3		
Session: Energy Conversion, Storage and Advanced Functional Materials	**Chair: Akrajas Ali Umar**	
09:00-09:25	**A12:** Disorder-Engineered High-Entropy Alloys for Broadband Metallic Acoustic Insulation	**Arup Neogi** University of North Texas, USA; Institute of Fundamental and Frontier Sciences, University of Electronic Science and Technology of China, China
09:25-09:50	**A13:** Engineering Morphology and Interfacial Properties of Silicide-Based Nanowires for Electrochemical Energy Storage and Magnetic Applications	**Goh Boon Tong** Universiti Malaya, Malaysia
09:50-10:15	**A14:** Surface Modification of Sputtered LCO Thin Films	**Nafarizal Nayan** Universiti Tun Hussein Onn Malaysia, Malaysia
10:15-10:35	**Coffee Break**	
10:35-11:00	**A15:** Enhancing the Hydrogen Evolution Reaction of Transition Metal Dichalcogenides via Metallic NbS_2 and Pt-MoS_2	**Abdul Rahman Mohmad** Institute of Microengineering and Nanoelectronics, Universiti Kebangsaan Malaysia, Malaysia
11:00-11:25	**A16:** Optimization of Electrodeposited n-Cu_2O Thin Film Using Etching and Annealing Technique	**Fariza Mohamad** Universiti Tun Hussein Onn Malaysia, Malaysia
11:25-14:00	**Lunch Break**	

Wednesday, 29 July 2026

Venue: Melur Hall at Level 3, Bangi Resort Hotel

Melur Hall at Level 3		
Session: Biomedical Engineering, Biosensing and Biological Systems Chair: Chang Fu Dee		
14:00-14:25	**A17:** 3D-Printed Biomedical Actuators and Sensors	**Yi Zhang** University of Electronic Science and Technology of China, China
14:25-14:50	**A18:** PeritoCare®: A Wearable Peritoneal Dialysis Device	**Azrul Azlan Hamzah** Institute of Microengineering and Nanoelectronics, Universiti Kebangsaan Malaysia, Malaysia
14:50-15:15	**A19:** A Multifunctional Nanoplatform for the Attenuation of Amyloid-β Fibrils	**Zhuo Zhang** Shimmer Center, Tianfu Jiangxi Laboratory; University of Electronic Science and Technology of China, China
15:15-15:35	**Coffee Break**	
15:35-16:00	**A20:** Design and Optimisation of Titanium Dioxide-Reduced Graphene Oxide Interdigitated Field-Effect Transistor for Biosensing Applications	Manal Ammar Institute of Microengineering and Nanoelectronics, Universiti Kebangsaan Malaysia, Malaysia
16:00-16:25	**A21:** Morphological and Strength Analysis of Lignocaine-Embedded Maltose-based Dissolvable Microneedles	**Arifah Syahirah Rahman** Institute of Microengineering and Nanoelectronics, Universiti Kebangsaan Malaysia, Malaysia
16:25–16:50	**A22:** Experimentally Profiling Dielectric Properties of Escherichia coli and Staphylococcus aureus by Movement Velocity and Force	**Muhamad Ramdzan Bin Buyong** Institute of Microengineering and Nanoelectronics, Universiti Kebangsaan Malaysia, Malaysia
16:50–17:15	**A23:** Investigation of Culturable Bacteria Associated with Medicinal Plants for Secondary Metabolite Profiling	**Purnima Neogi** School of Science, Engineering, and Technology, Penn State Harrisburg, USA

Thursday, 30 July 2026

Venue: Melur Hall at Level 3, Bangi Resort Hotel, Kuala Lumpur, Malaysia

China-Malaysia Future Industries & Innovation Cooperation Summit

Bilateral University-Research Institute Partnership Exchange

Slogan: Bridging Innovation and Education for Future Industries

Date	30 July 2026 (Thursday) | 9:00-16:00
Venue	Melur Hall at Level 3, Bangi Resort Hotel, Kuala Lumpur, Malaysia
Hosts	Universiti Kebangsaan Malaysia (UKM); Xihua University
Co-hosts	University of Electronic Science and Technology of China (UESTC); Tianfu Jiangxi Laboratory
Event Background	**Expected Outcomes**
To accelerate strategic partnerships in frontier technologies and joint talent cultivation, this summit brings together leading research institutions from China and Malaysia. The event focuses on quantum technology, embodied intelligence, integrated photonics, new energy, advanced materials, and future agriculture, while also addressing collaborative education models and talent exchange.	• Cooperation framework discussion and preliminary partnership intentions. • Joint research exploration in frontier fields including quantum technology, embodied intelligence, integrated photonics and advanced materials. • Education collaboration exchange on joint degree programmes, credit transfer mechanisms, and staff/student exchange schemes. • Talent programme consultation and matching of potential candidate resources. • In-depth networking through coffee breaks and lunch.

Summit Programme

Time	Program
09:00-09:15	Opening Remarks and Summit Introduction
09:15-10:00	Institutional Partnership Presentations by UKM, Xihua University, UESTC and Tianfu Jiangxi Laboratory
10:00-10:20	Coffee Break and Networking
10:20-11:30	Thematic Exchange: Future Industries and Frontier Technologies
11:30-12:30	Education Collaboration Dialogue and Talent Programme Consultation
12:30-14:00	Lunch and Networking
14:00-15:00	Research Partnership and MOU Discussion
15:00-15:20	Coffee Break and Networking
15:20-15:50	Summary of Cooperation Intentions and Follow-up Actions
15:50-16:00	Closing Remarks

Friday, 31 July 2026

Free Activities

Time	Program
Full day	Free activities / No scheduled conference activities

Poster Session

IMEN Colloquium 2026 – Interdisciplinary Forum Frontier Science 2026 (IFFS 2026)

Venue: Melur Hall at Level 3, Bangi Resort Hotel

Each poster presentation slot is 10 minutes.

Poster Session

Tuesday, 28 July 2026 | 13:30–16:50

Time	Poster Title	Presenter / Programme
13:30–14:00	**Registration**	
14:00–14:10	**P01**: Poster Title to be Confirmed	**Chunyu Li**
14:10–14:20	**P02**: Hydrothermal Synthesis of $NaYF_4$:Yb^{3+}/Er^{3+} Upconversion Microcrystals: Influence of Fluoride Concentration on Particle Crystallinity and Emission Intensity	**Yi Hong Lim**
14:20–14:30	**P03**: Ultra-responsive Piezoelectric Nanogenerators from Poly(vinylidene fluoride)/Poly(vinylidene fluoride-trifluoroethylene) Blends	**Rawhan Haque**
14:30–14:40	**P04:** Synthesis of 2-Dimensional NbS2 nanoflakes via NaCl-Assisted Chemical Vapor Deposition	**Mega Fatmasari** PhD
14:40–14:50	**P05:** Synthesis of Layer-Controlled MoS_2 by Chemical Vapor Deposition and Its Work Function Analysis Using KPFM	**Haque Rumman Mohammad Safiul** PhD
14:50–15:00	**P06:** Triboelectric Nanogenerator with Enhanced Output Performance Using PDMS/BTO/GQD Nanocomposite Materials for Energy Harvesting	**Faizatul Farah binti Hatta** PhD
15:00–15:10	**P07:** Enhancing the Phase Stability and Performance of FAPbI3 Perovskite Solar Cells via 4,4′-Oxydibenzenesulfonyl Chloride Additive Engineering	**Ikhwan Fikri Maulidan** DFAL
15:10–15:20	**P08:** Optimizing Laser-Induced Graphene Fabrication on Polyimide Substrates	**Muhammad Feidhul Hakim bin Fatah Yasin** PhD
15:20–15:30	**P09:** Optimizing the Rotor–Stator Air Gap in Non-Contact Rotating Triboelectric Nanogenerators via Finite-Element Analysis	**Govind A/L Maniam** PhD
15:30–15:40	**P10:** Differentiation of Escherichia coli and Staphylococcus aureus in Mixed Bacterial Suspensions Using Dielectrophoresis	**Muhammad Akmal bin Suhaimi** PhD
15:40–15:50	**P11:** Calibration of Dielectrophoretic Analytical Sensitivity as an Experimental Validation Parameter*	**Arash Zulkarnain bin Ahmad Rozaini** PhD
15:50–16:00	**P12:** Development of MoO3-x Based Saturable Absorber for Mode-Locked Erbium-Doped Fiber	**Muhammad Khairul Ashraf bin Azmi** MSc
16:00–16:10	**P13:** Poly(vinylidene fluoride) Nanocomposites Incorporating Graphene Quantum Dots and Magnesium Chloride for Piezoelectric Energy Harvesting	**Elyani Abu Bakar** PhD
16:10–16:20	**P14:** Cypermethrin Degradation on Chili Using an Air-Based Atmospheric Pressure Plasma Jet: Temporal Discharge Behaviour, Reactive Species, and Chemical Evidence	**Nur Ariena Hanis binti Mohd Nor** MSc

Time	Poster Title	Presenter / Programme
16:20–16:30	**P15:** Radio Frequency Energy Harvesting: Opportunities and Challenges	**Zaheer Abbas Balouch** PhD
16:30–16:40	**P16:** Effect of CeO_2 Addition on the Thermal Reliability of Pressureless Sintered Ag Joints	**Wang Weijie** PhD
16:40–16:50	**P17:** Metal-Free Isoxazoline-Indole Dual-Site Porous Polymer for 2,4,6-Trinitrotoluene Removal	**Wang Lun** PhD
16:50	**End of Session**	

Poster Session

Wednesday, 29 July 2026 | 13:40–16:50

Time	Poster Title	Presenter / Programme
13:40–14:10	**Registration**	
14:20–14:30	**P18**: Design and Optimisation of Titanium Dioxide-Reduced Graphene Oxide (TiO_2-rGO) Interdigitated Field-Effect Transistor (FET) for Biosensing Applications	**Manal Ammar**
14:30–14:40	**P19:** Polyvinylidene difluoride/Polyvinylidene difluoride-trifluoroethylene Hybrid Nanogenerator for Energy Harvesting	**Arthur Ling Wen Rong** MSc
14:40–14:50	**P20:** YOLO-to-Three-Dimensional Cutting PointLocalization for Robotic Oil Palm Harvesting	**Chan Shou Wei** MSc
14:50–15:00	**P21:** Two-Stage Deep Learning for Oil Palm Fresh Fruit Bunch Ripeness Classification and Harvest Prediction	**Elvin Yeoh Kang Shen** MSc
15:00–15:10	**P22:** Energy-Aware Multi-Robot Task Allocation for Autonomous Oil Palm Harvesting	**Wong Yi Chen** MSc
15:10–15:20	**P23:** Adaptive Motion Planning and Obstacle Handling for Autonomous Oil Palm Harvesting	**Alan Chung Shen Kai** MSc
15:20–15:30	**P24:** Engineering Interparticle Gap in ZnO Nanorods for Enhanced SERS Performance: A Simulation-Guided Approach for Creatinine Detection	**Izzah Hanaanah binti Ab. Aziz** PhD
15:30–15:40	**P25:** Simulation-Based Capacitive Micromachined Ultrasonic Transducers Detection of Pulmonary Embolism	**Hussnain Shahid** PhD
15:40–15:50	**P26:** Performance Enhancement of Diketopyrrolopyrrole-dithienothiophene-Based Organic Thin Film Transistors (OTFTs) Using Solvent Variation	**Reni Silvia Nasution** PhD
15:50–16:00	**P27:** Morphological and Strength Analysis of Lignocaine-Embedded Maltose-based Dissolvable Microneedles	**Arifah Syahirah binti Abdul Rahman** PhD
16:00–16:10	**P28:** Optimization of Fabrication Parameters for Calcium Chloride-Maltose-Sodium Alginate Dissolvable Microneedles Based on Hardness Evaluation by Nanoindentation	**Mohd Eusoff bin Azizul Nashriby** PhD
16:10–16:20	**P29:** Compact Dynamic Digital Frequency Divider Design for Low-Power Biomedical ADPLL Systems	**Abdul Khaliq** PhD
16:20–16:30	**P30:** Influence of Preparation Conditions on Phase Formation	**Nahrusyifa' binti Abdul**

Time	Poster Title	Presenter / Programme
	Hydrothermally Synthesized TiO2 Nanorods	**Karim** Phd
16:30–16:40	**P31:** Effect of Cu Substrate Surface Roughness on IMC Layer Growth Kinetics in Lead-Free Solder Joints	**Muhamad Nur Syahiran bin Muhamad Yusof** MSc
16:40–16:50	**P32:** The Effect of Silver Nanostars (AgNs) Layers as a SERS Substrate for Glucose Detection	**Nur Ain binti Mohd Nasir** MSc
16:50-17:00	**P33:** Effect of UV Post-Curing on Heavy Metal Rejection Performance of 3D-Printed Composite Membranes	**Noor Asnida Asli**
17:00-17:10	**P34:** Light-Driven Underwater Transport of Macroscale Soft Robots	**Dhriti Neogi**
17:10	**Award/Certificate Presentation, Group Photograph and Closing Session**	

ABSTRACT SESSION

A01: Quantum Many-Body Sensors

Abolfazl Bayat

University of Electronic Science and Technology of China

Exploiting quantum features allows for estimating external parameters with precisions well beyond the capacity of classical sensors, a phenomenon known as quantum-enhanced precision. While quantum criticality has been recognized as a resource for achieving such enhancements relative to probe size, it typically requires complex probe preparation and measurement and the achievable enhancement is ultimately restricted to narrow parameter regimes. On the other hand, non-equilibrium probes harness dynamics, enabling quantum-enhanced precision with respect to time over a wide range of parameters through simple probe initialization. Here, we unify these approaches through a Stark-Wannier localization platform, where competition between a linear gradient field and particle tunneling enables quantum-enhanced sensitivity across an extended parameter regime. We also provide experimental implementation of the proposal on a 9-qubit superconducting quantum device, where we explore its performance in the extended phase, the critical point and the localized phase. Despite employing only computational-basis measurements we have been able to achieve near-Heisenberg-limited precision by combining outcomes at distinct evolution times. In addition, we demonstrate that the performance of the probe in the entire extended phase is significantly outperforming the performance in the localized regime.

A02: Achieving Heisenberg Limit Under Noisy Conditions With Quantum Zeno Dynamics and Dynamical Decoupling

Ke Zeng[1], Yu Jiang[1], Bakmou Lahcen[1] and Kok Chuan Tan[1]

[1] *Institute of Fundamental and Frontier Sciences,*
University of Electronic Science and Technology of China, Chengdu 610051, China

Abstract: Quantum Zeno dynamics (QZD) and dynamical decoupling (DD) are powerful tools that enable the effective suppression of noise in quantum systems. We consider the problem of when (i) noise can be suppressed and (ii) Heisenberg limit (HL) can be achieved in quantum metrology, and prove necessary and sufficient conditions for when QZD and DD are useful for achieving these two goals. It is shown that the conditions for HL to be achievable using both methods are identical, and can be expressed succinctly as $H_S(\omega) \notin span\{S_i\}$, where $H_S = \omega G$ is the Hamiltonian encoding parameter ω onto the probe state and S_i are operators that describe the interaction with the environment. Finally, we demonstrate that the combination of both techniques can allow individually imperfect QZD and DD strategies to saturate.

A03: High-Precision Computational Reconstruction Integrated Spectroscopy Technology

Xue Tong

TianFu JiangXi Laboratory

Miniaturized spectrometer is currently undergoing rapid development. Such spectrometers can be deeply integrated with portable smart devices including smartphones and smart bracelets, boasting outstanding adaptability for diverse application scenarios. As a vital research branch of miniaturized spectrometers, computational reconstruction spectrometers extract light field information via micro-nano structures or optical units with designated wavelength responses, and reconstruct and restore incident spectra with the aid of algorithmic models.

Compared with conventional spectrometers, computational reconstruction spectrometers effectively break the mutual restriction bottleneck between device footprint and spectral resolution, demonstrating greater development potential. The number of detection channels serves as a core metric governing the key performance of computational reconstruction spectrometers. Conventional devices generally rely on dozens of detection channels for spectral sampling, which leads to insufficient spectral sampling, accompanied by drawbacks such as low spectral resolution, poor detection precision and limited detection bandwidth.

A04: Nanoscale Energy Converters: Bridging Optoelectronics and Photothermal Applications

Zhiming Wang

Tianfu Jiangxi Laboratory

Nanoscale materials serve as versatile platforms for efficient optical energy conversion. This presentation will showcase our recent work on two interconnected fronts, unified by the principle of tailored light-matter interactions.

First, I will discuss our advances in engineering semiconductor colloidal quantum dots (CQDs). Through rational design of core/shell structures and electronic band structures, we have developed CQDs with optimized carrier dynamics, broadband absorption, and enhanced stability for high-performance optoelectronic devices, including photodetectors and synaptic devices.

Building on this foundation, the talk will then explore how we leverage nanomaterials as efficient photothermal converters. We demonstrate the application of this concept in driving sophisticated processes in multifield optofluidics and environmental purification.

By unifying the realms of quantum-confined optoelectronics and photothermal energy conversion, our work highlights the broad potential of nanoscale designers in advancing future technologies for sensing, display, and beyond.

A05: Research and Development of High-Efficiency Semiconductor Optoelectronic Functional Materials, Device Integration and First-Principles Studies

Chengxin Zhou

Shimmer Center, Tianfu Jiangxi Laboratory

Semiconductor optofunctional materials constitute a critical foundation for the sustained evolution and transformation of modern society. Driven by the compelling pursuit of sustainable development and the accelerated advancement of new technological paradigms, the development of novel, high-efficiency semiconductor functional materials and devices has emerged as a strategic focal point for the reconfiguration of the global technology landscape and the enhancement of core competitiveness.

To address critical challenges in conventional semiconductor optofunctional materials and devices—including severe photogenerated carrier recombination, limited interfacial electric field effects, and the lack of synergy between light absorption and charge separation—this study adopts an integrated research

paradigm of first-principles calculation guidance, experimental precision fabrication, and device performance optimization. This approach enables accurate prediction of band structures, carrier dynamics, and defect behaviors, clarifies the regulatory mechanisms of atomic-scale interface engineering on performance, and systematically advances the controllable construction, microscopic mechanism analysis, device integration, and application exploration of high-efficiency optofunctional materials. For nonlinear optical materials, the introduction of electronegative groups is proposed to construct electric double layers and form polarization fields, thereby enhancing photogenerated carrier dynamics and thermodynamic properties. Interface perturbation engineering is employed to embed electron-withdrawing groups into non-centrosymmetric semiconductor surfaces, inducing pressure-stress-driven polyhedral distortion to generate macroscopic polarization. This strategy addresses the issue of facile electron-hole recombination caused by Coulombic forces while embedding electron transport media and acceptors to establish specialized electron transport pathways, resolving poor electron transport kinetics and effectively suppressing non-radiative carrier recombination. Furthermore, crystal facet regulation combined with oriented growth yields high-crystallinity semiconductor materials, which are integrated with surface plasmon resonance effects to enhance light capture capabilities. Gradient energy level heterojunctions and homoatomic bridging strategies are utilized to construct atomically intimate interfaces. Surface functional group modulation is applied to convert traditional Schottky contacts into Ohmic contacts, complemented by highly conductive media to reduce contact resistance, significantly advancing the comprehensive performance of semiconductor optofunctional materials.

A06: Development of High-Performance Organic Near-Infrared Upconversion Devices for Optoelectronic Signal Coordination and Biomedical Applications

Zeyu He [1]

[1]Shimmer Center, Tianfu Jiangxi Laboratory, Chengdu 641419, China

Near-infrared (NIR) detection and imaging technologies are critical for applications in biomedical imaging, optical communication, and national defense. Traditional inorganic NIR systems are costly and energy-intensive. Organic upconversion devices (UCDs) offer a promising alternative by enabling direct imaging without complex readout circuits, while leveraging the flexibility and high contrast of organic light-emitting devices (OLEDs). However, current organic UCDs face limitations such as low photon conversion efficiency, limited linear dynamic range, high driving voltages, and constrained performance in fluorescence-based systems.

To addressing these challenges, we precisely modulate intermolecular interactions and charge dynamics within UCDs to optimize energy transfer pathways and enhance carrier utilization. First, a ternary bulk heterojunction sensitized with an interfacial exciplex host and a phosphorescent emission module was developed, significantly improving energy conversion efficiency and lowering the turn-on voltage to 1.6 V. Second, optimization of the detection module’s structural design and film morphology led to a UCD with nearly 20% photon conversion efficiency and coordinated optoelectronic signal output, enabling high-precision arterial pulse monitoring and physiological imaging. Third, a novel Reverse-Distribution Phase Gradient Heterojunction (RP-GHJ) was constructed to suppress dark current density by three orders of magnitude, maintaining high contrast and detectivity under high bias for multi-wavelength biological imaging. Finally, a fluorescent emission module featuring a delayed fluorescent material with dual reverse intersystem crossing channels was designed, achieving external quantum efficiencies approaching 96.6% and demonstrating the viability of low-cost fluorescent materials for large-area UCDs.

By systematically refining exciton and carrier dynamics, this work establishes high-performance organic UCDs capable of synchronous optoelectronic output. The findings provide a foundation for future advancements in low-cost, flexible NIR detection and its translation into high-quality biomedical imaging and physiological monitoring applications.

A07: Controllable Preparation, Doping Modification, and Heterojunction Device Research of PbSe-Based Photodetection Materials

Silu Peng,

Shimmer Center, Tianfu Jiangxi Laboratory

Lead selenide (PbSe), as a narrow-bandgap semiconductor with excellent characteristics in the infrared region, still faces challenges in photodetector applications due to low carrier mobility, high dark current, and difficulties in nanoscale fabrication. This study focuses on improving the performance of PbSe-based photodetectors by systematically investigating controllable material preparation, elemental doping, and heterojunction construction. The main research contents are as follows: First, PbSe thin films were prepared using chemical bath deposition combined with iodine sensitization treatment, which effectively reduced the dark current, achieved a responsivity of 30.27 A/W at 808 nm, and successfully activated mid-infrared detection capability at 5000 nm. Second, high-quality PbSe nanosheets were fabricated via physical vapor deposition and subsequently formed into a p–n heterojunction with WSe_2. The resulting device achieved a responsivity of 15.6 A/W and a specific detectivity as high as 1.08×10^{11} Jones, with a response speed (511 μs/64 μs) three orders of magnitude faster than that of pure PbSe devices. Third, through a Te-doping strategy, PbSe0.5Te0.5 thin films were obtained, exhibiting a narrower bandgap and higher carrier mobility. A heterojunction device constructed with MoSe2 based on this material achieved broadband detection from 405 nm to 5000 nm, demonstrating a responsivity of 17.5 A/W, a specific detectivity of 3.08×1013 Jones, and an extremely low dark current of 0.72 pA. Finally, La doping was introduced to form Pb0.7La0.3Se, which further optimized the optical and electrical properties. A heterojunction device based on this material combined with WSe2 exhibited a responsivity of 22.85 A/W and response times of 162/135 μs. This study systematically validates the effectiveness of multiple strategies, including iodine sensitization, heterojunction design, and elemental doping, in enhancing the photoelectric performance of PbSe-based detectors. The responsivity, detectivity, and response speed of the devices have been significantly improved, and their detection spectral range has been effectively broadened. These findings provide a solid experimental foundation and new design insights for the development of high-performance, low-power infrared photodetectors.

A09: SERS for Detection and Biodetection

Ramon A Alvarez-Puebla

ICREA, Passeig Lluís Companys 23, 08010 Barcelona, Spain

Departamento de Quimica Fisica e Inorganica; Universitat Rovira i Virgili, Avda. Països Catalans 26, 43007 Tarragona, Spain

Email: ramon.alvarez@urv.cat

Surface-enhanced Raman scattering (SERS) is a powerful spectroscopic platform for chemical detection and biodetection because it combines molecular fingerprint specificity with signal amplification from plasmonic nanostructures. By engineering metallic nanoparticles, nanostructured substrates, encoded nanotags, and hybrid plasmonic materials, SERS can be adapted to detect a wide range of targets, including small molecules, proteins, biomarkers, pathogens, cells, and catalytic intermediates [1–8].

In biodetection, SERS offers important advantages over conventional optical and biochemical assays, including multiplexing, low limits of detection, compatibility with complex biological media, and the possibility of direct spectral identification. Plasmonic nanosensors have enabled ultrasensitive biomarker detection through signal-amplification strategies such as enzyme-guided nanocrystal growth [1]. Encoded SERS nanoparticles have also been used for multiplex bacterial identification in clinically relevant biofluid volumes, demonstrating the potential of SERS for rapid pathogen screening [2]. In parallel, SERS-based protein assays have allowed sensitive quantification of oncogenic biomarkers such as c-Jun and c-MYC in cellular extracts or real biological samples, illustrating the relevance of this technique for liquid biopsy and cancer-oriented diagnostics [3,4].

Beyond analytical quantification, SERS is increasingly becoming a tool for spatially resolved and dynamic biodetection. Holographic Raman microscopy has expanded SERS imaging toward three-dimensional localization and tracking of individual SERS probes in living cells [5]. Recent work on biomolecule-induced chiroptical responses in plasmonic assemblies further shows how molecular conformation, mechanics, and plasmonic coupling can be integrated into advanced optical biosensing concepts [6].

Finally, SERS is not limited to biological analysis. Hybrid plasmonic materials can also act as platforms for operando chemical detection, where the same nanostructure enhances Raman signals and participates in light-driven processes. Examples include plasmonic systems for monitoring photocatalytic nitrogen reduction and metal–organic framework-based plasmonic photocatalysts driven by hot-electron processes [7,8]. Overall, these developments show that SERS is a general and adaptable methodology for detection and biodetection, bridging analytical chemistry, nanophotonics, molecular diagnostics, bioimaging, and operando materials science.

A10: Low-Dimensional Materials: Synthesis, Characterization, Applications, and First-Principles Calculations

Chang-Fu Dee

Institute of Microengineering and Nanoelectronics (IMEN), The National University of Malaysia (Universiti Kebangsaan Malaysia, UKM), 43600, Bangi, Selangor, Malaysia

Various synthesis and fabrication techniques for low -dimensional structures have been developed to achieve high quality and low-cost production. One promising approach is the synthesis of silicon nanowires using hot-wire chemical vapor deposition (HWCVD) with an indium catalyst. In HWCVD, a heated tungsten filament decomposes silane and hydrogen gases, resulting in high-crystallinity silicon nanowires. The use of indium as a catalyst enables growth at relatively low temperatures due to its low melting point (157 °C), compared to conventional metals such as gold or copper. Key growth parameters, including catalyst size, filament temperature, substrate–filament distance, and deposition time, were optimized for improved nanowire formation. Subsequently, zinc oxide (ZnO) nanostructures were integrated onto the silicon nanowires to form three-dimensional heterostructured nanowires. ZnO was synthesized via vapor transport condensation and hydrothermal methods. These Si/ZnO heterostructures enhance the optical, photocurrent, and field emission properties of silicon nanowires, overcoming their inherent limitations.

Additionally, a ZnO nanorod-based field-effect transistor (FET) was developed as a human serum albumin (HSA) biosensor. A TiO_2-based interdigitated electrode (IDE) amperometric biosensor was also fabricated for detecting HSA and E. coli O157:H7. The TiO_2 nanoparticle platform enabled detection of HSA concentrations ranging from 1 mg/mL down to 1 pg/mL. Multiple devices were tested to assess stability, sensitivity, and reproducibility. After surface cleaning, the sensors demonstrated reusability with consistent I–V profiles across five devices, confirming reliable performance. Computational studies were conducted to complement the experimental findings. Molecular docking simulations were performed to analyze the structural and electrostatic characteristics of the antibody–antigen interface. The results confirmed that the APTES-functionalized TiO_2 IDE surface enhances antibody binding stability at pH 7, demonstrating the effectiveness of the TiO_2 platform for biosensor applications. These findings provide preliminary validation of the robust antibody immobilization on TiO_2 surfaces.

Additionally, first-principles calculations were carried out to investigate defects in various 2D and bulk materials. Structural stability, electronic properties, and electron localization were systematically analyzed. Using density functional theory (DFT), different phases of 2D $SnGe_2N_4$ were evaluated for catalytic water-splitting reactions. The computed reaction pathways and free-energy profiles indicate that $SnGe_2N_4$ is a promising photocatalyst for the oxygen evolution reaction (OER).

Keywords: Low-Dimensional Materials, Biosensors, Molecular Dynamics Studies, and First-Principles Calculations

A11: Enhancing Perovskite Solar Cells Stability via Additive（CANCELED）

Akrajas Ali Umar

Institute of Microengineering and Nanoelectronics, Universiti Kebangsaan Malaysia, 43600
Email: akrajas@ukm.edu.my (AAU).

Perovskite solar cells (PSCs) have emerged as leading candidates for next-generation photovoltaics owing to their low material cost, facile solution processing, tunable bandgaps and rapidly improving power conversion efficiencies. Among perovskite compositions, formamidinium lead iodide ($FAPbI_3$) delivers an ideal bandgap and enhanced thermal stability compared to methylammonium analogues, yet its photoactive α-phase undergoes undesirable conversion to the non-photoactive δ-phase at room temperature. Additive engineering has proven instrumental in overcoming this polymorphism by modulating crystallization kinetics, passivating defects and stabilizing the α-phase. Organic cations, inorganic dopants, ionic liquids and low-dimensional precursors each contribute complementary mechanisms multidentate coordination, hydrophobic surface capping, interfacial dipole formation and seed-assisted nucleation that synergistically enhance film quality, suppress nonradiative recombination and extend operational lifetimes under humidity, thermal and illumination stress. Structure–property relationships reveal that multifunctional additives achieve an optimal balance of efficiency and stability. This talk examines the role of the additive in absorber composition, classifies additive strategies by mechanistic function, stability metrics, and provides guidelines for translating laboratory advances into scalable, durable PSC architectures.

Keywords

Defects regulation; formamidinium lead iodide; additive engineering; perovskite solar cells; stability.

A12: Disorder-Engineered High-Entropy Alloys for Broadband Metallic Acoustic Insulation

Yuqi Jin[1] and Arup Neogi[1,2]

Department of Physics, University of North Texas, Denton, TX, 76210
Institute of Fundamental and Frontier Sciences, University of Electronic Science and Technology of China, Chengdu, PR China

Metals are essential for load-bearing structures, yet their efficient transmission of sound and vibration makes acoustic insulation difficult without adding bulky dampers or weakening the structure through engineered holes. This work presents a new strategy: using additive manufacturing–induced disorder as a functional design element rather than a defect.

Laser powder bed fusion was used to fabricate CrMnFeCoNi high-entropy alloy structures containing intrinsically formed, randomly distributed internal voids. These voids act as strong acoustic scatterers, producing multiple backscattering, destructive interference, and Anderson localization of ultrasonic waves. As a result, sound propagation is strongly suppressed across a broad frequency range without relying on narrow phononic bandgaps or added polymer damping layers. The printed high-entropy alloy samples achieved an average sound transmission reduction of approximately −65 dB across a 10 mm thickness, while retaining robust mechanical properties, including hardness about 10% higher than that of 316

stainless steel despite significant internal porosity. Numerical modeling confirmed exponential decay of acoustic intensity with a localization length of about 2.1 mm, establishing disorder-driven localization as the dominant insulation mechanism.

The impact of this work [1] lies in transforming porosity in metal additive manufacturing from an undesirable flaw into a scalable pathway for multifunctional structural materials. These disorder-engineered metallic acoustic insulators could enable compact, mechanically resilient sound-shielding components for aerospace systems, underwater structures, ultrasonic inspection, advanced manufacturing, and vibration-sensitive platforms. This approach opens a new materials-design paradigm in which strength, manufacturability, and broadband acoustic insulation are integrated into a single printed metallic architecture.

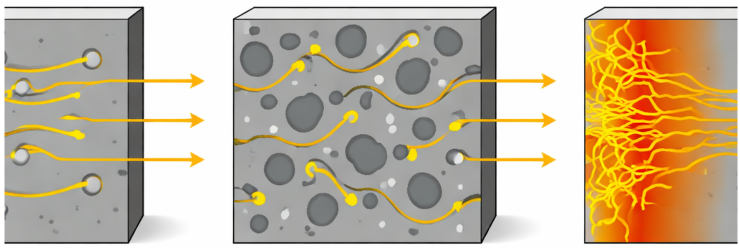

[1] Jin, Y., Kumar, J., Palaniappan, S. *et al.* Laser-powder bed fusion printed CrMnFeCoNi high entropy alloys engineered for acoustic insulation. *Commun Eng* **5**, 85 (2026). https://doi.org/10.1038/s44172-026-00624-5

A13: Engineering Morphology and Interfacial Properties of Silicide-Based Nanowires for Electrochemical Energy Storage and Magnetic Applications

Xiaoxi Li[a], Boon Tong Goh[a*], Keat Hoe Yeoh[b], Yee Hui Robin Chang[c]

[a]*Low Dimensional Materials Research Centre, Department of Physics, Faculty of Science, Universiti Malaya,50603, Kuala Lumpur, Malaysia*

[b]*Jeffrey Sachs Center on Sustainable Development, Sunway University, Bandar Sunway, 47500, Petaling Jaya,Selangor Darul Ehsan, Malaysia*

[c]*Faculty of Applied Sciences, Universiti Teknologi MARA, Cawangan Sarawak, Kota Samarahan, Sarawak, 94300,Malaysia*

One-dimensional (1D) metallic and semiconducting nanowires have emerged as promising materials for energy storage and conversion due to their large surface-to-volume ratios, tunable electronic properties, and excellent electrochemical performance. In this work, we have developed a diverse set of 1D nanowires, including single-crystal silicon and silicide nanowires, as well as a variety of core–shell heterostructures, using custom made CVD vacuum systems. Metallic silicide nanowires such as Ni_3Si and Mn_4Si_7, along with their heterostructures (e.g., Ni_3Si_2/Si and Ni_2Si/SiC), exhibit highly uniform, high-aspect-ratio morphologies and dense surface-active sites. These properties contribute to strong electrochemical behavior, as demonstrated by a Ni_3Si_2 nanowire/activated-carbon asymmetric supercapacitor that achieved high specific capacity, notable energy and power densities, and good cycling stability, effectively bridging the performance gap between traditional batteries and supercapacitors. Additional functionalities were also observed; for example, Mn_4Si_7 nanowires exhibited room-temperature ferromagnetism, while Ni_2Si/SiC core–shell nanowires showed enhanced electrical conductivity and improved electrochemical durability compared to intrinsic Si and SiC nanowires. Collectively, these advances highlight the broad potential of engineered 1D nanowire architectures for use in next-generation nanoelectronic and energy-related devices.

Keywords: Nanowires, Ni_3Si_2, Mn_4Si_7, Electrochemical Supercapacitor, Ferromagnetism

A14: Surface Modification of Sputtered LCO Thin Films

Nafarizal Nayan, Noor Kamalia Binti Abd Hamed, Riyaz Ahmad Bin Mohamed Ali, Silambarasan Kuppusamy, Mohd Khairul Bin Ahmad

Universiti Tun Hussein Onn Malaysia

Megat Muhammad Ikhsan Megat Hasnan

Universiti Malaya, Kuala Lumpur, Malaysia

Chrisminder Dain, Chong Jia Cherng

Petronas Research Sdn Bhd, Bangi, MalaysiaIn this project, Lithium Cobalt Oxide (LiCoO2 or LCO) thin films have been successfully deposited and modified for the purpose to evaluate their potential for advanced energy storage. While LCO remains a mainstream cathode material for commercial battery devices due to its high volumetric energy density and excellent conductivity, conventional electrodes are reaching their performance limits. To overcome these limitations, the project proposed a novel approach utilizing a quantum tunneling effect induced by nanoscale surface modifications to significantly enhance battery charging and discharging capabilities. Researchers utilized Radio Frequency (RF) magnetron sputtering to deposit ultra-thin LCO layers—ranging from 8.5 nm to 50 nm—onto substrates such as nickel sheets and nickel foam, a method chosen for its ability to yield high crystallinity and smooth surfaces. The deposited films subsequently underwent post-deposition surface modifications to create nanostructures, specifically through thermal annealing at temperatures like 200°C and reactive ion etching for 2 minutes. Galvanostatic Charge/Discharge (GCD) testing revealed that reducing the film thickness drastically improved performance; an ultra-thin 8.5 nm film (deposited for 5 minutes) achieved a specific capacitance of 455 F/g, reflecting a 65% improvement over a thicker 50 nm film. Furthermore, modifying the surface via thermal annealing at 200°C yielded a unique surface pattern with a maximum specific capacitance of 635.25 F/g and a specific energy density of 50.82 Wh/kg, marking a substantial 88% improvement over untreated samples. Ultimately, Conductive Atomic Force Microscopy (C-AFM) measurements validated the quantum tunneling concept, as the nanostructured LCO/Nickel samples exhibited significant "ripple" behavior in their nano-scale current-voltage (I-V) curves—indicative of a tunneling effect—which was absent in pure nickel samples, successfully proving that these structural modifications uniquely facilitate electron tunneling and transport at room temperature.

A15: Enhancing the Hydrogen Evolution Reaction of Transition Metal Dichalcogenides via Metallic NbS_2 and Pt-MoS_2

Abdul Rahman Mohmad

Institute of Microengineering and Nanoelectronics, Universiti Kebangsaan Malaysia, Bangi 43600, Selangor, Malaysia

Using hydrogen as an energy carrier offers a promising pathway to address global sustainability, energy security, and CO_2 emission challenges. However, the electrochemical reduction of protons to generate hydrogen relies heavily on expensive platinum catalysts. While two-dimensional transition metal dichalcogenides (TMDs) have emerged as potential low-cost alternatives, their practical application remains hindered by low density of active sites and low electrical conductivity. This work reports two distinct strategies to overcome these limitations: developing metallic TMDs and doped TMDs. In the first strategy, metallic NbS_2 flakes were synthesized via salt-assisted chemical vapor deposition (CVD) using sulfur and a mixture of Nb_2O_5 and NaCl precursors. The resulting NbS_2 flakes exhibited lateral dimensions up to 60 µm and thicknesses of ~100 nm. Raman spectroscopy revealed that the flakes were either a 3R

phase or a mixed 2H/3R phase, depending on the growth conditions. Characterization data suggest a vapor-liquid-solid (VLS) growth mechanism, in which the reaction between Nb_2O_5 and NaCl produces a liquid-phase Na_xNbO_y intermediate that subsequently undergoes sulfurization to form NbS_2. In the second strategy, the hydrogen evolution reaction (HER) performance of MoS_2 was enhanced by electrochemically dispersing platinum nanoparticles onto its surface. CVD-grown MoS_2 flakes on glassy carbon substrates were subjected to cyclic voltammetry (CV) in an acidic electrolyte, varying the cycle number from 250 to 1500. The Pt-modified MoS_2 exhibited significantly higher HER activity, characterized by a low overpotential, a small Tafel slope, and a markedly reduced charge-transfer resistance compared to pristine MoS_2. X-ray photoelectron spectroscopy (XPS) confirmed that continuous electrochemical cycling also induced partial oxidation of the MoS_2 and promoted the formation of PtS species. These strategies offer valuable insights for obtaining highly efficient HER catalysts.

A16: Optimization of Electrodeposited n-Cu_2O Thin Film Using Etching and Annealing Technique

Nurliyana Mohamad Arifin[1], Fariza Mohamad[2,3*], Sharmela d/o Sundar[4], Mohd Zamzuri Mohammad Zain[5], Masanobu Izaki[6]

[1]School of Engineering and Computing, MILA University, Putra Nilai, 71800 Nilai, Negeri Sembilan Malaysia

[2]Faculty of Electrical and Electronic Engineering, Universiti Tun Hussein Onn Malaysia (UTHM), 86400, Parit Raja, Batu Pahat Johor, Malaysia

[3]Microelectronic and Nanotechnology Shamsuddin Research Centre (MiNT-SRC), UTHM

[4]Intel Microelectronics (m) Sdn Bhd, Bayan Lepas Industrial Park, Pulau Pinang, Malaysia

[5]Faculty of Mechanical Engineering Technology, Universiti Malaysia Perlis, Arau, Perlis, Malaysia

[6]Department of Electrical Engineering, National Institute of Technology, Nara College, Japan

**Corresponding e-mail: farizamd@uthm.edu.my*

Cuprous oxide (Cu_2O) is one of metal oxide semiconductor materials that use in fabrication thin film for solar cell application. This study focuses on the analysis of n-Cu_2O thin films with respect to post-deposition treatments, specifically hydrothermal etching and annealing durations. The n-Cu_2O films were fabricated on fluorine-doped tin oxide (FTO) coated glass substrates using the electrodeposition technique, carried out for 30 minutes at 60°C. Post-deposition process involved hydrothermal etching at 150°C for 3 hours using diluted ethanol, followed by annealing at 200°C for durations of 20, 40, and 60 minutes. The successful fabrication of n-Cu_2O was confirmed by the presence of characteristic diffraction peaks corresponding to the (111) crystal orientation, exhibiting the highest intensity at 36.4°. Morphological analysis appeared densely packed with well-defined facets and rosette-like shapes, indicating optimal crystallinity and uniformity. The surface roughness and resistivity decreased significantly after 40 minutes of annealing duration, reaching 50.319 nm and 0.13 Ω/cm, respectively. From the characterization results, the sample annealed for 40 minutes exhibited optimal performance. In conclusion, these findings confirm that the combination of hydrothermal etching and optimized annealing significantly improves the quality of n-Cu_2O thin films for potential photovoltaic applications. *(192 words)*

A17: 3D-Printed Biomedical Actuators and Sensors

Yi Zhang[1,2]

[1]School of Integrated Circuit Science and Engineering, University of Electronic Science and Technology of China, Chengdu, Sichuan, China;

[2] *School of Medicine, University of Electronic Science and Technology of China, Chengdu, Sichuan, China.*

ft magnetic millirobots hold significant promise for noninvasive surgery, drug delivery, and point-of-care diagnostics, yet traditional fabrication methods like molding and 2D lithography cannot produce complex 3D structures, and conventional vat photopolymerization (VP) suffers from severe magnetic particle sedimentation, leading to inhomogeneous composites, low loading ratios, and weak magnetic responses. This work presents Circulating Vat Photopolymerization (CVP), an innovative 3D printing approach that integrates a recirculating mixing system into stereolithography (SLA) to continuously homogenize magnetic particle–resin composites during printing. The CVP system circulates the resin–particle mixture between the vat and a mixing chamber, effectively suppressing particle settling; characterization via density measurements and EDX elemental mapping confirms uniform magnetic particle distribution in printed parts, in sharp contrast to the graded, nonuniform distribution in standard VP prints.

This method enables magnetic particle loading up to 30% (w/v), yielding robust magnetic responsiveness and large deformations in soft millirobots. Using CVP, the authors successfully fabricated multifunctional 3D magnetic soft millirobots with intricate architectures, including grippers, caterpillar-like robots, rocking horses, and jellyfish-shaped devices. Under controlled magnetic fields, these millirobots execute diverse droplet manipulation tasks—transport, merging, ejection, splitting, and synchronized pushing—and can perform remote point-of-care testing for potentially biohazardous pathogens. CVP offers a rapid, scalable route to fabricate versatile, magnetically controlled soft millirobots, expanding their capabilities for biomedical and microfluidic applications.

This talk covers recent work in Prof. Yi Zhang's group, including 3D-printed biomedical magnetic millirobots, 3D-printed microneedle sensor and drug delivery system, and other related topics.

A18: PeritoCare®: A Wearable Peritoneal Dialysis Device

Azrul Azlan Hamzah

Institute of Microengineering and Nanoelectronics, Universiti Kebangsaan Malaysia, Malaysia

PeritoCare® is a portable peritoneal dialysis system, which has been developed since 2018. Development and Human Clinical Trial of PeritoCare® is funded by the Ministry of Science, Technology and Innovation (MOSTI), Malaysia, and is a collaborative development between Institute of Microengineering and Nanoelectronics (IMEN), Universiti Kebangsaan Malaysia, the Faculty of Medicine, Universiti Kebangsaan Malaysia and Peritoneal Dialysis Unit, Hospital Canselor Tuanku Muhriz, Malaysia. PeritoCare® is designed to ease End-stage kidney disease (ESKD) patients to perform dialysis on-the-go, while doing their daily routines. PeritoCare® is a portable dialysis device equipped with various sensors and designed for mobility. The oldest patient involved with the human clinical trial is 71 years old and the youngest is 21 years old. The first PeritoCare® clinical trial was performed on 8th of October 2020 and the final trial was performed on the 27th of June 2022. Majority of the patients have multiple comorbidities. The patients involved in this study were diagnosed with ESKD of various etiology and the commonest cause of ESKD in Malaysia is due to diabetes mellitus. Patients' peritoneal dialysis regime were prescribed by the doctors. Some of the patients needed 2000 ml dialysate and some need up to 2500 ml dialysate. As a conclusion of the trial, 82% of the tested patients agreed and strongly agreed to use PeritoCare® in the future for their dialysis treatment. This shows that the human clinical trial of PeritoCare® was a success. PeritoCare® received Malaysian Medical Device Authority (MDA) full certification on 30th June 2023.

A19: A Multifunctional Nanoplatform for the Attenuation of Amyloid-β Fibrils

Zhuo Zhang[1,2]

[1]*Shimmer Center, Tianfu Jiangxi Laboratory, Chengdu 641419, China;*

[2]*School of Physics, University of Electronic Science and Technology of China, Chengdu 610054, China.*

The abnormal amyloid-β (Aβ) aggregation is critical in the progression of Alzheimer's disease pathology, yet clinical therapeutics to alleviate amyloidosis in the patients is hindered due to low efficiency and side effects. Here, a multifunctional nanoplatform (PFs@E/P/S), where Aβ targeting peptide KLVFFA, small-molecule EGCG and superparamagnetic iron oxide nanoparticles (SPIONs) were combined together to attenuate Aβ fibrils, alleviate Aβ fibrils-induced cytotoxicity, and function as an MRI probe, is reported. Specifically, PFs@E/P/S enables Aβ targeting through the hydrogen bond of the KLVFFA component. Meanwhile, Aβ fibrils were attenuated by hydrogen bond and electrostatic interactions, thereby alleviating Aβ fibrils-induced reactive oxygen species (ROS) and mitochondrial dysfunction as well as membrane damage further. In addition, PFs@E/P/S also exhibited favorable blood compatibility, biosafety as well as BBB permeability in vivo. Of note, the combination of SPIONs enables PFs@E/P/S as a potential MRI probe. It is expected that multifunctional PFs@E/P/S provides an attractive avenue to promote the development of precise and efficacious treatment of Alzheimer's disease.

A20: Design and Optimisation of Titanium Dioxide-Reduced Graphene Oxide Interdigitated Field-Effect Transistor for Biosensing Applications

Manal Ammar[1] Sharipah Nadzirah[1] Farahdiana Wan Yunus[1] Azrul Azlan Hamzah[1]

[1]Institute of Microengineering and Nanoelectronics, Universiti Kebangsaan Malaysia, Malaysia

Titanium dioxide (TiO_2) and reduced graphene oxide (rGO) have attracted significant interest in biosensing applications owing to their complementary properties, including high biocompatibility, large surface area, excellent electrical conductivity, and enhanced charge transport characteristics. The integration of these materials into field-effect transistor (FET)-based biosensors offers promising opportunities for developing highly sensitive and miniaturised sensing platforms. In particular, the incorporation of interdigitated electrode (IDE) structures can improve electric field distribution and increase the effective sensing area, potentially enhancing device performance. This study presents the design and optimisation of a titanium dioxide-reduced graphene oxide (TiO_2-rGO) interdigitated field-effect transistor (IDE-FET) biosensor through numerical simulation and statistical optimisation techniques. A TiO_2-rGO-based IDE-FET structure was designed and modelled using COMSOL Multiphysics, and a conceptual fabrication procedure is proposed to support future experimental realisation. The effects of key design parameters, namely channel spacing, source and drain electrode width, gate electrode width, TiO_2-rGO thickness, and SiO_2 thickness, were investigated using a Taguchi L25 orthogonal array design of experiments (DOE). Signal-to-noise ratio (SNR) analysis and analysis of variance (ANOVA) were employed to determine the significance of each parameter and identify the optimal device configuration. The optimisation study revealed that SiO_2 thickness exerted the greatest influence on device performance, contributing 29.47% to the overall variation, followed by source and drain electrode width and channel spacing. The optimisation process identified an IDE-FET configuration capable of achieving a drain current of 121 nA. A confirmation simulation verified the reliability of the predicted optimum configuration. The findings demonstrate the potential of TiO_2-rGO IDE-FET architectures for biosensing applications and provide valuable design guidelines for the development of high-performance FET-based biosensors. The proposed optimisation framework may facilitate the efficient design of next-generation nanomaterial-based biosensing platforms.

Keywords: interdigitated electrode, biosensor, TiO_2-rGO, field-effect transistor, sensitivity

A21: Morphological and Strength Analysis of Lignocaine-Embedded Maltose-based Dissolvable Microneedles

Arifah Syahirah Rahman

Institute of Microengineering and Nanoelectronics, Universiti Kebangsaan Malaysia, Malaysia

Microneedles is a minimally invasive transdermal drug delivery system that can address some limitations of conventional topical formulations and hypodermic needles. In this study, lignocaine-loaded maltose dissolving microneedle arrays were fabricated and evaluated based on formulation, morphology, and mechanical performance. Suitable formulation was established during mould filling process to ensure reproducible microneedle formation, before being observed under FESEM and tested for mechanical strength using texture analyzer (TA). Field-emission scanning electron microscopy showed that the fabricated microneedles had sharp tips and relatively uniform geometry. Mechanical testing using a texture analyzer was performed to assess whether the microneedles could withstand compression during application. Overall, the selected maltose–lignocaine formulation showed suitable processability, acceptable structural integrity, and adequate mechanical robustness. These findings suggest that maltose based dissolving microneedles have potential as a platform for minimally invasive local anesthetic delivery.

Keywords: dissolvable; microneedle; lignocaine; maltose; texture analyzer; scanning electron microscopy

A22: Experimentally Profiling Dielectric Properties of Escherichia coli and Staphylococcus aureus by Movement Velocity and Force

Akmal Suhaimi[1,5], Arash Zulkarnain[1,5], Noraziah Mohamad Zin[2], Abdullah Abdulhameed[3], Aminuddin
Ahmad Kayani[4] & Muhamad Ramdzan Buyong[1,5*]

[1]*Institute of Microengineering and Nanoelectronics (IMEN), Universiti Kebangsaan Malaysia, Bangi 43600, Selangor, Malaysia.*

[2]*Centre for Diagnostic, Therapeutic and Investigative Studies Faculty of Health Sciences Universiti Kebangsaan Malaysia Jalan Raja Muda Abdul Aziz, 50300 Kuala Lumpur, Malaysia.*

[3]*Centre for Communication Systems and Sensing, King Fahd University of Petroleum and Minerals, 31261 Dhahran, Saudi Arabia.*

[4]*Functional Materials and Microsystems Research Group and the Micro Nano Research Facility, RMIT University, Melbourne, Australia.*

[5]*Akmal Suhaimi, Arash Zulkarnain and Ramdzan Buyong have equally contributed to this work.*

**email: muhdramdzan@ukm.edu.my*

The gradual research in integrating artificial intelligence in the Dielectrophoresis system is rapid since the evolution of AI in every aspect of technology since the early 2020s. The benefits of AI integration into DEP systems include improving position and accuracy, faster processing and decision-making, enhancing particle classification, reducing human error, and many others. On the other hand, DEP research often focuses on CMF values of the particles. CMF values explain the behavior of the particle under the influence of the electric force in terms of trajectory and force magnitude. CMF values are calculated from the equation that requires the conductivity and permittivity of the medium and particles. One important aspect of CMF values is that they are non-numerical. Although possible, it is difficult to develop an algorithm using non-numerical values for detection applications. Hence, the study will focus on translating the non-numerical CMF values of *E. coli* and *S. aureus* into velocity (meters per second) and force (Newtons) parameters. In this study, we develop a simple method of calculating velocity and force units of bacterial movement using pixel coordinates and the time frame of the recorded video. From there, we managed to plot a force and velocity curve experimentally, with a crossover frequency of 1.0 to 1.5 MHz for *S. aureus* bacteria and 500 to 600 kHz for *E. coli* bacteria. Then, we validated our results with the velocity and force curves extracted from COMSOL simulation and the CMF curve extracted from MYDEP simulation. Our results show that the experimental curve plotted agrees with the simulation curve plotted from the COMSOL simulation, and the crossover frequency plotted in the experiment agrees with the CMF curve from MYDEP. The conclusion of the study is that the method developed in the study is important as the first step for the development of an artificial intelligence system to be integrated into the DEP system. The additional parameter of velocity alongside crossover frequency will improve the detection accuracy of

bacterial cells using DEP technology. Furthermore, the collective data from future studies using this method will push DEP technology for future benefits.

A23: Investigation of Culturable Bacteria Associated with Medicinal Plants for Secondary Metabolite Profiling

Purnima Neogi[1], Aratrika Chakrabarti[1], Boktor, Jonathan[3] and Veronica Roman-Reyna[2]

[1]School of Science, Engineering, and Technology, Penn State Harrisburg, PA;

[2]Department of Plant Pathology and Environmental Microbiology, University Park, PA.

Medicinal plants are important sources of bioactive compounds with significant therapeutic value, and many modern pharmaceuticals have originated from plant-derived molecules. Increasing evidence also suggests that plant-associated microbiomes may contribute to the biosynthesis or control of these bioactive metabolites. In this study, we investigate the culturable bacterial communities associated with two medicinal plant species native to Pennsylvania, Echinacea purpurea and Hypericum prolificum. E. purpurea is widely recognized for its immunomodulatory and anti-inflammatory properties and for its traditional use in reducing respiratory infections, whereas H. prolificum is known for its antimicrobial and anti-inflammatory activities.

The objective of this research is to isolate genomic DNA from the leaves of both plant species and characterize their culturable bacterial populations, including both endophytic and epiphytic communities. Bacterial isolates will be cultured, and their DNA will be extracted, sequenced, and taxonomically analyzed to identify the dominant bacterial genera associated with each host plant. This work aims to provide insight into the diversity of plant-associated bacteria and their potential relationships to the medicinal properties of these species. By establishing a foundation for linking culturable microbiome composition with secondary metabolite potential, this study is likely to contribute to a broader understanding of plant–microbe interactions in medicinal plants. The findings can support future efforts in natural product discovery, microbiome-assisted agriculture, and the development of novel therapeutic resources.

ABSTRACT SESSION FOR POSTER

P01: Polarization Photovoltage Transistor Enabling Amplified Responsivity and Sensitivity

Authors and Affiliations

Authors

Jiayue Han†, Fakun Wang†, **Chunyu Li**†, Wenjie Deng, Shi Zhang, Libo Zhang, Fangchen Hu, Zhen Wang, Hongxi Zhou, He Yu, Jun Gou, Zhiming Wu, Zhiming Wang, Yadong Jiang, Qi Jie Wang*, Jun Wang*

Affiliations

1. School of Optoelectronic Science and Engineering, University of Electronic Science and Technology of China, Chengdu, China
2. State Key Laboratory of Electronic Thin Films and Integrated Devices, University of Electronic Science and Technology of China, Chengdu, China
3. Center for OptoElectronics and Biophotonics, School of Electrical & Electronic Engineering, Nanyang Technological University, Singapore
4. Shimmer Center, Tianfu Jiangxi Laboratory, Chengdu, China
5. School of Physics, University of Electronic Science and Technology of China, Chengdu, China
6. Key Laboratory of Optoelectronics Technology, Ministry of Education, Faculty of Information Technology, Beijing University of Technology, Beijing, China
7. College of Physics and Optoelectronic Engineering, Hangzhou Institute for Advanced Study, University of Chinese Academy of Sciences, Hangzhou, China
8. Zhangjiang Laboratory, Shanghai, China
9. State Key Laboratory of Infrared Physics, Shanghai Institute of Technical Physics, Chinese Academy of Sciences, Shanghai, China
10. School of Physical and Mathematical Science, and Photonics Institute, Nanyang Technological University, Singapore

† Equal contribution: Jiayue Han, Fakun Wang, Chunyu Li

* Corresponding authors: qjwang@ntu.edu.sg; wjun@uestc.edu.cn

---

Background / Introduction

Mid-infrared photodetectors are important for all-day, non-contact sensing because MIR radiation can penetrate complex environments and provide information beyond visible and near-infrared detection. When polarization sensitivity is introduced, MIR detectors can simultaneously capture thermal radiation and polarization contrast, which is valuable for intelligent security, environmental monitoring, autonomous driving, biomedical diagnostics, de-fogging, de-camouflage, and polarization communication.

However, conventional MIR polarization detection generally relies on division-of-focal-plane architectures, micro-optical components, and cooling systems, making device miniaturization and on-chip integration difficult. Two-dimensional materials offer a compact and filter-free route, but many anisotropic 2D materials suffer from weak intrinsic optical anisotropy, with polarization ratio often below 10. Existing approaches can increase PR, but usually at the expense of responsivity, noise, or response speed. Therefore, achieving high PR, high responsivity, and fast response simultaneously remains a key challenge for MIR polarization detection.

Objectives

This work aims to:

1. Develop a mid-infrared polarization photovoltage field-effect transistor based on BP/MoS_2 van der Waals heterostructures.
2. Integrate polarization detection and electrical amplification within a single device architecture.
3. Use gate-tunable transconductance to amplify polarization-dependent photovoltage response.
4. Improve polarization ratio without sacrificing responsivity and response speed.
5. Demonstrate high-precision MIR linear polarization angle discrimination and imaging.

Methods

Device design

The device is constructed as a BP/MoS_2 polarization photovoltage field-effect transistor. BP acts as the anisotropic MIR absorber, while MoS_2 serves as the conduction channel. The BP/MoS_2 interface forms a type-II heterojunction, where the polarization-dependent photovoltage modulates the depletion region and controls the source-drain channel current.

Device fabrication

MoS_2 and BP flakes were mechanically exfoliated from bulk crystals. Graphene-coated Au electrodes were used to form a clean MoS_2 channel. BP was transferred onto the MoS_2 channel and connected to the Au electrode as the top junction gate. The device was fabricated on a SiO_2/highly doped Si substrate under nitrogen atmosphere and encapsulated with hBN. The MoS_2 channel thickness was approximately 5.5 nm, and the BP absorber thickness was approximately 51 nm.

Characterization and measurement

Polarized Raman spectroscopy, FTIR absorption spectroscopy, optical microscopy, AFM, and cross-sectional TEM were used to characterize materials and device structure. The optoelectronic properties were measured under 3.5 μm MIR illumination using a semiconductor analyzer, optical parametric oscillator laser, MIR half-wave plate, and optical chopper. Noise spectral density and time-resolved photoresponse were also measured.

Simulation

TCAD simulations were used to analyze the carrier dynamics, energy band modulation, depletion-region variation, and gate-controlled electrostatic field effect in the BP/MoS_2 PPFET.

Results and Discussion

1. Device mechanism

The BP/MoS_2 heterostructure generates anisotropic photovoltage under MIR illumination. This photovoltage modulates the depletion width of the MoS_2 channel, similar to a junction field-effect transistor. The photoresponse is mainly governed by the light-induced photovoltage and the gate-tunable transconductance, rather than direct photocarrier injection.

2. Polarization amplification

By tuning the junction-gate voltage, the device operating point can be selected within different amplification regimes. The nonlinear evolution of transconductance stretches the polarization-dependent response curve, thereby enhancing PR while maintaining responsivity and speed.

3. Key performance metrics

The device achieved:

Parameter	Value
Illumination wavelength	3.5 μm
Maximum polarization ratio	~510
Electrically tunable PR range	~8.4 to ~510
Polarization angle sensitivity	~46.57 mA/(W·degree)
Responsivity at optimized angular discrimination point	~2.67 A/W

Parameter	Value
Peak responsivity	~6.9 A/W
Specific detectivity	~1.87 × 10^9 Jones
Response time	~0.8 µs
Simulated -3 dB bandwidth	>10^8 Hz

The results indicate that an extremely high PR alone does not necessarily produce the best angle discrimination. At $V_{tgs} = -0.1$ V, the PR is slightly lower than the maximum value but the responsivity is higher, resulting in the best PAS. This shows that balancing PR and responsivity is more important than simply maximizing PR.

4. Polarization imaging demonstration

The device was used as a single-pixel MIR polarization detector to scan a shadow mask. The "MIR" pattern carried different polarization information, including 0°, 5°, and 90°. Compared with the BP control device, the PPFET showed clearer discrimination among different polarization states and better extinction behavior. A four-pixel polarization imaging strategy was further used to reconstruct Stokes parameters, DoLP, and AoLP. For an initial polarization angle of approximately 40°, the reconstructed AoLP was about 39.88°, showing high accuracy in linear polarization angle discrimination.

Conclusion

A BP/MoS_2 mid-infrared polarization photovoltage field-effect transistor was demonstrated. By combining anisotropic photovoltage generation with gate-tunable field-effect amplification, the device simultaneously improves polarization ratio, responsivity, and response speed. The PPFET achieves a PR up to ~510, PAS up to ~46.57 mA/(W·degree), and response time down to ~0.8 µs under 3.5 µm illumination. These results show that PPFETs provide a promising platform for high-performance, compact, and high-precision MIR polarization detection and imaging.

Future Work / Outlook

The work suggests several future directions:

1. Twist-engineered PPFETs for reconfigurable polarization detection

Introducing twisted van der Waals heterostructures may further modulate interfacial symmetry, band alignment, and anisotropic photovoltage generation, enabling electrically reconfigurable linear and circular polarization responses.

2. Bipolar-channel PPFETs for multimodal infrared sensing

Replacing the MoS_2 channel with bipolar or ambipolar 2D materials may allow gate-controlled polarity switching, supporting multimodal detection that integrates intensity, wavelength, polarization, and photocurrent direction information.

3. Mechanism extension toward intelligent multidimensional optoelectronics

The photovoltage-field-effect amplification strategy could be extended to other anisotropic absorbers and infrared heterostructures, providing a device-level platform for high-sensitivity polarization sensing, optical encoding, and intelligent infrared perception.

References

1. Han, J., Wang, F., Li, C. et al. Polarization Photovoltage Transistor enabling Amplified Responsivity and Sensitivity. *Nature Communications* 2026. DOI: 10.1038/s41467-026-71444-6.

2. Tong, L. et al. Stable mid-infrared polarization imaging based on quasi-2D tellurium at room temperature. *Nature Communications* 11, 2308, 2020.

3. Han, J. et al. Mid-Infrared Bipolar and Unipolar Linear Polarization Detections in Nb_2GeTe_4/MoS_2 Heterostructures. *Advanced Materials* 35, 2305594, 2023.

4. Dai, M. et al. Long-wave infrared photothermoelectric detectors with ultrahigh polarization sensitivity. *Nature Communications* 14, 3421, 2023.

5. Bullock, J. et al. Polarization-resolved black phosphorus/molybdenum disulfide mid-wave infrared photodiodes with high detectivity at room temperature. *Nature Photonics* 12, 601–607, 2018.

6. Wang, F. et al. 2D computational photodetectors enabling multidimensional optical information perception. *Nature Communications* 16, 6791, 2025.

Acknowledgements

This work was supported by the National Key Research and Development Program of China, National Natural Science Foundation of China, Singapore Agency for Science, Technology and Research, National Research Foundation Singapore, China Postdoctoral Science Foundation, and Tianfu Jiangxi Laboratory. Specific grants include 2023YFB3611400, 62305013, 62305047, R23I0IR041, M23M2b0056, NRF-CRP29-2022-0003, NRF-MSG-2023-0002, 2025M780794, and TFJX-ZD-2025-014.

Contact / QR Code

Corresponding authors

Qi Jie Wang: qjwang@ntu.edu.sg
Jun Wang: wjun@uestc.edu.cn

Co-authors:

Chunyu Li: lichunyu@jxl.ac.cn

P02: Hydrothermal Synthesis of $NaYF_4$:Yb^{3+}/Er^{3+} Upconversion Microcrystals: Influence of Fluoride Concentration on Particle Crystallinity and Emission Intensity

Yi Hong Lim[1], Son-Qian Liew[1], Huei Ling Ching[1] and Kok-Keong Chong[1*]

[1] Lee Kong Chian Faculty of Engineering and Science, Universiti Tunku Abdul Rahman, Bandar Sungai Long, 43000 Kajang, Selangor, Malaysia

Abstract. Lanthanide-doped upconversion nanoparticles (UCNPs) exhibit unique optical properties that make them suitable for a wide range of applications. However, hydrothermal synthesis of sodium-based rare-earth-doped UCNPs often yields particles with limited crystallinity and mixed morphologies, requiring extended reaction times to obtain high-quality β-$NaYF_4$. In this work, hydrothermal synthesis was employed to produce β-$NaYF_4$:Yb^{3+}/Er^{3+} upconversion microparticles (UCMPs), which, while larger than conventional UCNPs, serve as an effective model system for investigating the fundamental effects of fluoride concentration on crystal growth, phase purity, and optical properties. Scanning electron microscopy revealed no significant change in overall particle size distribution with increasing fluoride concentration. In contrast, X-ray diffraction and photoluminescence measurements demonstrate a clear enhancement in crystallinity and upconversion emission intensity at higher fluoride concentrations. When the fluoride amount used increased from 84 mmol to 104 mmol, the 521 nm and 655 nm emission peaks increased from 0.081 to 0.142 a.u. and 0.329 to 0.495 a.u., respectively. These results suggest that fluoride primarily influences crystal growth and defect reduction rather than particle size under the investigated conditions. This study provides insight into optimizing fluoride conditions for the synthesis of highly crystalline and optically efficient UCMPs via hydrothermal method.

Keywords: Upconversion microparticles, $NaYF_4$:Yb^{3+}/Er^{3+}, Hydrothermal synthesis, morphology, crystallinity, upconversion intensity, fluoride concentration, microprisms

*Corresponding author: chongkk@utar.edu.my

P03: Ultra-responsive Piezoelectric Nanogenerators from Poly(vinylidene fluoride)/Poly(vinylidene fluoride-trifluoroethylene) Blends

Rawhan Haque[1], Poh Choon Ooi[1]

[1] Institute of Microengineering and Nanoelectronics (IMEN), Universiti Kebangsaan Malaysia, 43600 Bangi, Selangor, Malaysia

Corresponding author: pcooi@gmx.com (Poh Choon Ooi)

Abstract

Enhancing the β-phase content of poly(vinylidene fluoride) (PVDF) remains a key challenge for improving its piezoelectric performance in flexible energy harvesting applications. In this work, a polymer blending strategy was employed by incorporating poly(vinylidene fluoride-trifluoroethylene) (PVDF-TrFE) into PVDF to promote β-phase formation through intermolecular interactions, chain alignment, and lattice modification induced by TrFE incorporation. Unlike conventional approaches that rely on mechanical stretching, electrical poling, or filler incorporation, the proposed blending method provides a simple and effective route for tailoring the crystalline phase and electrical response of PVDF-based materials. The influence of PVDF-TrFE content on phase evolution, crystallinity, and piezoelectric behavior was systematically investigated. Structural analyses confirmed that blending PVDF with PVDF-TrFE effectively suppressed amorphous regions and promoted enhanced β-phase formation compared with pristine PVDF and previously reported blend systems. Morphological observations further revealed disrupted spherulitic growth and improved structural ordering, which contributed to enhanced electrical performance. Among the investigated compositions, the optimized PVDF:PVDF-TrFE (1:2) blend exhibited superior piezoelectric output, delivering an open-circuit voltage of 14.7 V, a short-circuit current of 1.5049 ± 0.01 µA, and a maximum power density of 16.15 µW/cm². The device also generated 4.0 V under a low applied force of 0.2 N, demonstrating excellent sensitivity under weak mechanical stimuli. The obtained electrical output was sufficient to power low-energy microsensor nodes, including commercial motion sensors and ultra-low-power radar modules, highlighting the feasibility of the blend system for self-powered electronics, Internet of Things devices, soft robotics, and wearable sensing applications. This study demonstrates that PVDF/PVDF-TrFE blending is an effective and scalable strategy for enhancing β-phase crystallinity and piezoelectric performance in flexible polymer-based energy systems.

P04: Synthesis of 2-Dimensional NbS2 nanoflakes via NaCl-Assisted Chemical Vapor Deposition

Mega Fatmasari

Programme: PhD

NaCl-Assisted Chemical Vapor Deposition

Abstract

The synthesis of thin and high-quality niobium disulfide (NbS_2) flakes on SiO_2/Si substrates is technologically challenging. In this study, we report the synthesis of NbS2 using a single zone chemical vapor deposition (CVD) system which uses sulfur and a mixture of Nb2O5 and NaCl as the precursors. The alkali metal salt (NaCl) acts as a growth promoter by lowering the melting point of the Nb2O5. The effects of growth parameters on the growth of NbS2 flakes such as the amount of NaCl, gas flow rate, growth time and temperature were systematically investigated. Based on the results, the optimum growth conditions are 20 mg of NaCl, 60 sccm of Ar/H2 gas flow rate, and substrate heated at 800°C for 30 minutes. The Raman spectra show vibrational modes of NbS2 while AFM indicates an average flake thickness of 46 nm. The XPS spectra indicate that the sample has a high density of S vacancies due to a low S-toNb ratio of 1.6.

Keywords: NbS_2, chemical vapor deposition, controllable synthesis, salt-asisted CVD, growth parameters

P05: Synthesis of Layer-Controlled MoS_2 by Chemical Vapor Deposition and Its Work Function Analysis Using KPFM

Haque Rumman Mohammad Safiul

Programme: PhD

Abstract

This study explores a systematic experimental investigation of the layer-dependent electronic work function of large-area MoS_2 synthesized by chemical vapor deposition (CVD). High-quality films with controlled thicknesses, ranging from monolayer to few-layer, were grown using MoO_3 and sulfur precursors under optimized furnace conditions. Structural and compositional characterization was performed via Raman spectroscopy, AFM, TEM/SEM, and XPS. Kelvin probe force microscopy (KPFM), calibrated against Au references, was employed to obtain quantitative work function maps. Our measurements reveal a consistent increase in work function with layer number, rising by ~0.1–0.2 eV between monolayer and ~10-layer MoS_2, in agreement with prior reports. This trend is attributed to enhanced screening of substrate-induced charge transfer and adsorbate effects in thicker films. Error sources including tip calibration, surface inhomogeneity, and environmental adsorbates are analyzed. These findings highlight the critical role of thickness in tuning MoS_2 electronic properties, with direct implications for contact engineering and band alignment in device applications. Future studies will focus on environmental control and substrate engineering to further modulate MoS_2 surface potential.

Keywords: TMDC, KPFM, Work Function, MoS2

P06: Triboelectric Nanogenerator with Enhanced Output Performance Using PDMS/BTO/GQD Nanocomposite Materials for Energy Harvesting

Faizatul Farah binti Hatta

Programme: PhD

Abstract

Triboelectric nanogenerators (TENGs) have been developed as promising energy-harvesting devices to effectively convert mechanical energy into electricity. TENGs use either organic or inorganic materials to initiate the triboelectrification process, followed by charge separation. In this study, a high-performance composite-based triboelectric nanogenerators (CTENGs) device was fabricated, comprising polydimethylsiloxane (PDMS a) as a polymeric matrix, barium titanite (BTO) nano-powders as dielectric fillers and graphene quantum dot (GQD) as conductive media. The PDMS/BTO/GQD composite film was prepared with the GQD doped into the mixture of PDMS/BTO and mechanically stirred. The composition of GQD varied from 0 to 40 wt%. The composite was spin-coated onto flexible ITO on a PET sheet and dried in the oven at 80°C for 24 hours. The output performance of TENGs is enhanced by the increased concentration of 30 wt% GQD, which is two times higher than nanocomposite films without GQD. The PDMS/BTO/G30 TENGs film depicted an increase in open-circuit voltage output (VOC), short-circuit current output (ISC) and power density reaching ~310.0 V, ~23.0 µA and 1.6 W/m2 respectively. The simple and scalable process for the PDMS/BTO/GQD TENGs would benefit as a sustainable energy harvesting system in small electronic devices.

Keywords: nanogenerators, triboelectric nanogenerators, energy harvesting, nanocomposite graphene

P07: Enhancing the Phase Stability and Performance of FAPbI3 Perovskite Solar Cells via 4,4′-Oxydibenzenesulfonyl Chloride Additive Engineering

Ikhwan Fikri Maulidan

Programme: DFAL

Abstract

Formamidinium lead triiodide ($FAPbI_3$) perovskite solar cells (PSCs) represent a premier front in next-generation photovoltaics due to an optimal bandgap of approximately 1.48 eV. However, pristine $FAPbI_3$ is hindered by thermodynamic instability at room temperature, easily undergoing a spontaneous polymorphic phase transition from the photoactive black phase to the non-perovskite yellow phase under ambient environmental exposure. To circumvent these microstructural limitations, 4,4′-oxydibenzenesulfonyl chloride (OBSC) is introduced as a multi-functional molecular mediator designed to regulate crystallization kinetics and comprehensively passivate deep-level electronic defects. The structural architecture of OBSC incorporates dual sulfonyl chloride ($-SO_2Cl$) functional groups that exhibit strong electronic affinity for undercoordinated Pb^{2+} sites and organic FA^+ cations, while its flexible ether-linked backbone provides an adaptable configuration capable of bridging multiple adjacent lead defect sites across grain boundaries. Consequently, OBSC stabilizes the perovskite-solvent adduct during film deposition, slowing nucleation to deliver highly crystalline films. Planar n-i-p devices configured with an optimized 0.5 mg concentration of OBSC achieved a champion power conversion efficiency (PCE) of 17.4726%. This substantial enhancement is driven by an extraordinary inflation of the short-circuit current density (JSC) to 53.2 mA/cm2 and an improved fill factor (FF) of 0.4264, despite an interfacial dipole-induced shift that compresses the open-circuit voltage (VOC) to 0.7703 V. Furthermore, the unencapsulated OBSC-treated device retained 47.32% of its initial efficiency after 240 hours of continuous ambient testing (30 ± 5% relative humidity), a retention capability significantly higher than that of the pristine control device, which degraded to 34.43% of its initial capacity within just 168 hours.Ultimately, this additive engineering strategy provides a highly effective and structurally sound pathway for developing efficient and operationally durable perovskite solar cells.

Keywords: formamidinium lead iodide, additive engineering, perovskite solar cells, stability.

P08: Optimizing Laser-Induced Graphene Fabrication on Polyimide Substrates

Muhammad Feidhul Hakim bin Fatah Yasin

Programme: PhD

Graphene’s progress as a wonder material is hindered by constrictive fabrication parameters such as high temperature, vacuum environment and harsh chemicals. Laser-Induced Graphene (LIG) offers a scalable, single-step approach for converting polyimide (PI) into conductive porous graphene networks under ambient conditions. This study investigates the coupled effects of CO_2 laser (10.6μm) power (10–17 W) and scan speed (20–100 mm/s) on electrical, structural, and morphological properties of LIG. Results reveal a diagonal thermal processing window where optimal conductivity (≈27–32 Ω) is achieved through coordinated increases in power and scan speed, with a minimum resistance of 26.96 Ω at 16 W and 60 mm/s. Raman analysis confirms reduced defect density within this regime, while SEM shows a hierarchical porous structure supporting both conductivity and mechanical stability. However, operation near the lower resistance limit approaches the ablation threshold, risking film degradation, whereas insufficient energy leads to non-conductive regions. A balanced condition (15 W, 80 mm/s) provides an optimal trade-off between electrical performance and structural integrity. These findings establish key process constraints for reproducible and scalable LIG fabrication.

Keywords: laser-induced graphene, polyimide, CO2 laser, electrical response, porous graphene.

P09: Optimizing the Rotor–Stator Air Gap in Non-Contact Rotating Triboelectric Nanogenerators via Finite-Element Analysis

Govind A/L Maniam

Programme: PhD

Abstract

Triboelectric nanogenerators (TENGs) convert ambient motion into electricity for self-powered electronics. In non-contact rotating TENGs (NCR-TENGs), the rotor–stator separation is a key design choice governing the trade-off between mechanical durability and electrostatic output. This work builds a 3D finite-element electrostatic model of a segmented NCR-TENG in COMSOL Multiphysics to examine how the air gap affects the electric potential distribution, open-circuit voltage, and induced effective charge density. An effective dielectric thickness framework represents the rotor–stator assembly, and the gap is swept from 0 to 8 mm with all other parameters fixed. A wider gap raises the effective dielectric thickness, lowering capacitance and electrostatic induction, so charge density and output voltage fall steadily. A usable 3–5 mm range is recommended, over which the open-circuit voltage stays near 530–650 V and the effective charge density near 1–1.35 μC m−2. These results offer early guidance for air gap selection in durable non-contact rotating TENGs.

Keywords: triboelectric nanogenerator, non-contact rotating, energy harvesting, COMSOL, air gap

P10: Differentiation of Escherichia coli and Staphylococcus aureus in Mixed Bacterial Suspensions Using Dielectrophoresis

Muhammad Akmal bin Suhaimi

Programme: PhD

Abstract

Rapid identification of bacterial species is important for clinical diagnostics, infection control, and environmental monitoring. Conventional microbiological methods often require lengthy culture and biochemical analyses, which can delay pathogen identification. In this study, dielectrophoresis (DEP) was investigated as a rapid and label-free technique for differ-entiating bacterial species in mixed suspensions. Two clinically relevant bacteria, Escherichia coli and Staphylococcus aureus, representing Gram-negative and Gram-positive organisms, re-spectively, were used as model species. Bacterial suspensions were prepared in a medium with controlled conductivity of 0.03 S/m to ensure consistent DEP conditions. Mixed bacterial samples were prepared using different dilution ratios to vary the relative cell concentrations. In Mixture A, E. coli was diluted at 1:100 and S. aureus at 1:1000, while in Mixture B, the dilution ratios were reversed. DEP experiments were conducted at two selected frequencies, 150 kHz and 400 kHz, based on previously characterized responses of the two species. At 150 kHz, both bacteria experienced negative DEP and were differentiated based on velocity response. At 400 kHz, differentiation was based on particle trajectory and separation behavior. For each experiment, 100 particles were tracked and classified based on their DEP response. At 150 kHz, the expected dominant species was detected at 64.33 ± 3.06% in the E. coli-rich mixture and 67.00 ± 10.58% in the S. aureus-rich mixture. At 400 kHz, detection improved to 86.00 ± 7.55% for the E. coli-rich mixture and 75.00 ± 7.55% for the S. aureus-rich mixture. These results demonstrate that DEP can differentiate E. coli and S. aureus in mixed bacterial suspensions, with trajectory-based separation at 400 kHz providing clearer differentiation than velocity-based analysis at 150 kHz. The findings highlight the potential of DEP as a rapid, label-free, and reagent-free approach for bacterial screening in clinical diagnostics and environmental monitoring.

P11: Calibration of Dielectrophoretic Analytical Sensitivity as an Experimental Validation Parameter*

Arash Zulkarnain bin Ahmad Rozaini

Programme: PhD

Abstract

Dielectrophoresis (DEP) has emerged as a promising label-free technique for rapid bacterial manipulation and detection. However, experimental validation of DEP response is commonly performed through particle velocity measurements, which become increasingly unreliable for bacterial-scale particles due to Brownian motion, imaging limitations, and particle heterogeneity. This study proposes analytical sensitivity as an alternative population-based experimental parameter for validating DEP behaviour. Structural characteristics of Acinetobacter baumannii were obtained using transmission electron microscopy (TEM), revealing a bacterial diameter of 658.3 nm, cell wall thickness of 17.2 nm, and membrane thickness of 12.2 nm. These parameters were incorporated into a MyDEP dielectric model to simulate the frequency-dependent Clausius–Mossotti factor, Re[CM(f)], and compared with literature-derived dielectric properties.DEP experiments were subsequently performed between 0.1 and 3 MHz using titanium interdigitated microelectrodes.Analytical sensitivity was defined as the percentage of bacterial cells exhibiting observable DEP motion relative to the total bacterial population within a tandardized region of interest. Experimental results demonstrated a strong agreement between analytical sensitivity and theoretical dielectric polarization, yielding a correlation coefficient of $r = 0.933$. Furthermore, TEM-derived dielectric parameters provided improved agreement with experimental observations compared with literature-based models, highlighting the importance of structural characterization in DEP simulations. The highest analytical sensitivity was observed at 3 MHz under positive DEP conditions (82%), whereas the strongest negative DEP response occurred at 0.1 MHz (97%). These findings establish analytical sensitivity as a practical experimental bridge between DEP theory and observable bacterial behaviour, providing a quantitative framework for DEP validation and frequency optimization in bacterial biosensing applications.

Keywords: Dielectrophoresis, analytical ensitivity, Correlation

P12: Development of MoO3-x Based Saturable Absorber for Mode-Locked Erbium-Doped Fiber

Muhammad Khairul Ashraf bin Azmi

Programme: MSc

Abstract

This study presents the development of a sub-stoichiometric molybdenum trioxide (MoO3-x) based saturable absorber (SA) synthesized using the hot-wire chemical vapor deposition (HWCVD) technique and its application in an erbium-doped fiber laser (EDFL). Material characterization confirmed the formation of MoO3-x structures with oxygen vacancies that contribute to enhanced nonlinear optical properties. The developed MoO3-x-SA was incorporated into the EDFL cavity, resulting in stable dual-wavelength mode-locking operation with picosecond pulse generation. These findings demonstrate the potential of MoO3-x as an effective saturable absorber for ultrafast fiber laser applications.

Keywords: Sub-stoichiometric molybdenum trioxide, saturable absorber, mode-locking, erbium-doped fiber laser.

P13: Poly(vinylidene fluoride) Nanocomposites Incorporating Graphene Quantum Dots and Magnesium Chloride for Piezoelectric Energy Harvesting

Elyani Abu Bakar

Programme: PhD

Abstract

This study demonstrated that incorporating $MgCl_2$ into graphene GQD-reinforced PVDF nanocomposites effectively enhanced the structural ordering and piezoelectric performance of flexible nanogenerators. The optimized device achieved a Voc of 4.81 Vp-p, an Isc of 941.43 nA, and a maximum power density of 5.7 $\mu W\ cm^{-2}$ across a 500 kΩ load while maintaining stable performance over four months of continuous operation. These findings demonstrate the potential of the proposed nanocomposite for flexible energy-harvesting and self-powered electronic applications.

Keywords: Piezoelectric nanogenerator, Poly(vinylidene fluoride), Graphene quantum dots, Nanofillers, Magnesium chloride, β-phase

P14: Cypermethrin Degradation on Chili Using an Air-Based Atmospheric Pressure Plasma Jet: Temporal Discharge Behaviour, Reactive Species, and Chemical Evidence

Nur Ariena Hanis binti Mohd Nor

Programme: MSc

Abstract

This study investigates the use of an air-based atmospheric pressure plasma jet (APPJ) for cypermethrin decontamination on chili (Capsicum annuum L.) through four coordinated analyses. Temporal discharge power measurements at 18 kV and 3 L/min showed a linear increase from 6.34 to 15.07 mW over 2–10 minutes ($R^2 = 0.95$), attributed to progressive dehumidification of the compressed air supply, establishing a 10-minute warm-up recommendation. Optical emission spectroscopy confirmed generation of N2 SPS, N2+ FNS, and atomic oxygen species under the same condition. LC-MS/MS quantification demonstrated up to 59% cypermethrin removal at 18 kV/3 L/min after 2 minutes with 10 minutes plasma warm up. ATR-FTIR spectroscopy confirmed bond-level chemical degradation through the reduction of the ester carbonyl band (1729 cm-1), emergence of a new carboxylate band at 1419 cm-1 as evidence of ester cleavage products, and preservation of the chili matrix peaks throughout.

Keywords: APPJ, cypermethrin, discharge power, OES, FTIR, chili

P15: Radio Frequency Energy Harvesting: Opportunities and Challenges

Zaheer Abbas Balouch

Programme: PhD

Abstract

The surge of the Internet of Things (IoT) in smart farming has facilitated the mass adoption of sensor networks for monitoring soil, crops, livestock, and environmental parameters. A notable limitation of this paradigm is its reliance on batteries, which pose significant challenges for maintenance, cost, and environmental sustainability, particularly in large or remote agricultural areas. Radio Frequency Energy Harvesting (RFEH) has emerged as a compelling strategy for achieving sustainable, battery-independent or battery-augmented operation of low-power agricultural sensors. This study presents a systematic investigation of a microstrip patch antenna (MPA) designed for integration into radio-frequency energy harvesting (RFEH) systems for smart farming applications. The proposed antenna operates within the 2.4 GHz ISM band and achieves a notable gain of 2.78 dBi. Furthermore, it achieves efficient impedance matching, with a reflection coefficient below -10 dB. This study highlights persistent operational difficulties, including low energy densities achievable through RFEH, signal propagation matching in rural landscapes, and design constraints imposed by the pursuit of energy independence in sensor networks. This study outlines the opportunities and challenges of RFEH in agriculture, aiming to inform ongoing research and enhance resilient, environmentally sustainable smart farming systems.

Keywords: RF energy harvesting, smart farming, RFEH, low power sensors, battery-less, sustainable energy

P16: Effect of CeO_2 Addition on the Thermal Reliability of Pressureless Sintered Ag Joints

Wang Weijie

Programme: PhD

Abstract

Pressureless sintered silver joints were investigated as die-attach materials for high-temperature electronic packaging. However, their reliability was limited by pore coarsening, interfacial degradation, and crack propagation during thermal loading. In this study, Ag and Ag-1%CeO2 joints were compared to evaluate the effect of CeO2 addition on thermal reliability. Ce was uniformly distributed in the Ag-1%CeO2 joint. After 500 h thermal aging at 250 °C, Ag-1%CeO2 joint showed a more stable porous structure than Ag joint. This result indicated that CeO2 nanoparticles acted as pinning sites and suppressed pore coarsening during aging. After 600 thermal shock cycles, Ag joint showed obvious interfacial degradation. In contrast, Ag-1%CeO2 changed the damage behavior from interfacial delamination to distributed internal microcracking. This crack deflection process required higher fracture energy and delayed rapid interfacial failure. SAM results further confirmed slower defect evolution in the Ag-1%CeO2 joint. These results suggested that 1 wt.%CeO2 addition improved the microstructural stability and thermal reliability of pressureless sintered Ag joints.

Keywords: Sintered silver; CeO2; Pressureless sintering; Thermal aging; Thermal shock.

P17: Metal-Free Isoxazoline-Indole Dual-Site Porous Polymer for 2,4,6-Trinitrotoluene Removal

Wang Lun

Programme: PhD

Abstract

Efficient removal of 2,4,6-trinitrotoluene (TNT) from contaminated water remains challenging due to the limited availability of adsorbents with cooperative adsorption sites. In this work, a metal-free isoxazoline-indole dual-site porous polymer was synthesized through nitrile oxide click polymerization followed by freeze-drying. The polymer integrates isoxazoline N-O dipolar sites and indole π-rich planes within a porous framework, enabling cooperative TNT adsorption. Owing to its dual-site adsorption mechanism and porous mass-transfer network, the polymer achieved a maximum TNT adsorption capacity of 295.6 mg g^{-1} at 298 K and reached 74% of its maximum capacity within 1 h. The adsorbent also exhibited good recyclability and maintained stable performance during repeated adsorption-desorption cycles. These findings demonstrate the potential of metal-free dual-site porous polymers for efficient TNT removal from water.

Keywords: 2,4,6-trinitrotoluene; Porous organic polymer; Metal-free click polymerization; Isoxazoline-indole polymer; Dual-site adsorption.

P18: Design and Optimisation of Titanium Dioxide-Reduced Graphene Oxide (TiO_2-rGO) Interdigitated Field-Effect Transistor (FET) for Biosensing Applications

Manal Ammar[1] Sharipah Nadzirah[1] Farahdiana Wan Yunus[1] Azrul Azlan Hamzah[1]

[1]Institute of Microengineering and Nanoelectronics, Universiti Kebangsaan Malaysia, Malaysia

ABSTRACT

Titanium dioxide (TiO_2) and reduced graphene oxide (rGO) have attracted significant interest in biosensing applications owing to their complementary properties, including high biocompatibility, large surface area, excellent electrical conductivity, and enhanced charge transport characteristics. The integration of these materials into field-effect transistor (FET)-based biosensors offers promising opportunities for developing highly sensitive and miniaturised sensing platforms. In particular, the incorporation of interdigitated electrode (IDE) structures can improve electric field distribution and increase the effective sensing area, potentially enhancing device performance. This study presents the design and optimisation of a titanium dioxide-reduced graphene oxide (TiO_2-rGO) interdigitated field-effect transistor (IDE-FET) biosensor through numerical simulation and statistical optimisation techniques. A TiO_2-rGO-based IDE-FET structure was designed and modelled using COMSOL Multiphysics, and a conceptual fabrication procedure is proposed to support future experimental realisation. The effects of key design parameters, namely channel spacing, source and drain electrode width, gate electrode width, TiO_2-rGO thickness, and SiO_2 thickness, were investigated using a Taguchi L25 orthogonal array design of experiments (DOE). Signal-to-noise ratio (SNR) analysis and analysis of variance (ANOVA) were employed to determine the significance of each parameter and identify the optimal device configuration. The optimisation study revealed that SiO_2 thickness exerted the greatest influence on device performance, contributing 29.47% to the overall variation, followed by source and drain electrode width and channel spacing. The optimisation process identified an IDE-FET configuration capable of achieving a drain current of 121 nA. A confirmation simulation verified the reliability of the predicted optimum configuration. The findings demonstrate the potential of TiO_2-rGO IDE-FET architectures for biosensing applications and provide valuable design guidelines for the development of high-performance FET-based biosensors. The proposed optimisation framework may facilitate the efficient design of next-generation nanomaterial-based biosensing platforms.

Keywords: interdigitated electrode, biosensor, TiO_2-rGO, field-effect transistor, sensitivity

P19: Polyvinylidene difluoride/Polyvinylidene difluoride-trifluoroethylene Hybrid Nanogenerator for Energy Harvesting

Arthur Ling Wen Rong

Programme: MSc

Abstract

Hybrid triboelectric–piezoelectric nanogenerators have attracted increasing attention for mechanical energy harvesting. This work investigates polyvinylidene difluoride (PVDF) and polyvinylidene difluoride-trifluoroethylene (PVDF-TrFE) composite films as active layers for hybrid nanogenerators. Devices with different PVDF:PVDF-TrFE blend ratios were fabricated and evaluated under periodic mechanical excitation. Among the investigated compositions, the PVDF:PVDF-TrFE ratio of 1:2 exhibited the highest electrical performance, generating 13.8 V open-circuit voltage and 6.9 µA short-circuit current. The results demonstrate that PVDF:PVDF-TrFE blending is an effective approach for enhancing the electrical output of hybrid triboelectric–piezoelectric nanogenerators for energy harvesting applications.

Keywords: Polyvinylidene difluoride, polyvinylidene difluoride-trifluoroethylene, hybrid nanogenerator, triboelectricity, piezoelectricity.

P20: YOLO-to-Three-Dimensional Cutting PointLocalization for Robotic Oil Palm Harvesting

Chan Shou Wei

Programme: MSc

Abstract

Conventional red-green-blue (RGB) vision systems for robotic oil palm harvesting often struggle with cutting-point localization under dense foliage, severe occlusion, and variable outdoor illumination. This work presents a computationally efficient You Only Look Once (YOLO)-to-three-dimensional (3D) perception framework that integrates YOLOv8 instance segmen-tation on near-infrared (NIR) intensity images with synchronized Time-of-Flight (ToF) 3D sensing. Segmented targets are directly mapped to 3D

point clouds for spatial localization, followed by geometric refinement using principal component analysis (PCA) and Random Sample Consensus (RANSAC)-based cylinder fitting to estimate cutting vectors for Fresh Fruit Bunch (FFB) stems and frond petioles. Field validation on a custom Robot Oper-ating System 2 (ROS 2)-based harvesting platform deployed in Malaysian oil palm plantations achieved detection accuracies of 96.78% (box) and 96.50% (mask), mean Average Precision at an Intersection-over-Union (IoU) threshold of 0.5 (mAP50) values of 98.45% and 98.19%, respectively, and a 3D localization root mean square error (RMSE) of 3.2 cm. More than 100 harvesting trials demonstrated a 91% clean-or-acceptable success rate while maintaining real-time operation at up to 30 frames per second (FPS) on edge hardware.

Index Terms—Robotic oil palm harvesting, YOLOv8 instance segmentation, cutting-point localization, near-infrared imaging, Time-of-Flight sensing.

P21: Two-Stage Deep Learning for Oil Palm Fresh Fruit Bunch Ripeness Classification and Harvest Prediction

Elvin Yeoh Kang Shen

Programme: MSc

Accurate maturity assessment of oil palm fresh fruit bunches (FFBs) is essential for optimizing oil yield, yet conventional manual inspection is subjective and unsuitable for large-scale deployment. This study presents a two-stage deep learning framework that integrates You Only Look Once version 8 segmentation (YOLOv8-seg) instance segmentation with a Real-Time Detection Transformer (RT-DETR) classifier for four-category FFB ripeness grading based on exocarp colour percentage. The segmentation stage isolates FFBs from complex plantation backgrounds through pixel-level masking, while the RT-DETR classifier captures both local fruitlet texture and global colour distribution. Evaluated using five-fold cross-validation, the framework achieves 95.94% accuracy, 95.93% F1-score, and 99.66% Receiver Operating Characteristic– Area Under the Curve (ROC-AUC), outperforming benchmark architectures. The system operates at 8–18 Frames Per Second (FPS), demonstrating suitability for real-time autonomous harvesting applications. This progress report summarizes the current model development and preliminary evaluation.

Keywords: oil palm fresh fruit bunch (FFB); ripeness classification; instance segmentation; RT-DETR; deep learning; precision agriculture

P22: Energy-Aware Multi-Robot Task Allocation for Autonomous Oil Palm Harvesting

Wong Yi Chen

Programme: MSc

Abstract

Autonomous multi-robot harvesting in oil palm plantations requires efficient task allocation under energy-constrained field conditions. This study proposes a hierarchical framework integrating the Consensus-Based Bundle Algorithm (CBBA) with a State-Adaptive Memetic Particle Swarm Optimisation (SAM-PSO) scheduler. The proposed SAM-PSO employs an Evolutionary State Estimation (ESE)-driven elitist 2-Opt refinement mechanism to mitigate premature convergence and improve route quality. The framework was evaluated on a simulated plantation containing 587 harvest targets under battery-swap constraints and benchmarked against Particle Swarm Optimisation (PSO), Ant Colony Optimisation (ACO), Zebra Optimisation Algorithm (ZOA), and a greedy nearest-neighbour (GREEDY-NN) heuristic. Results from 30 independent replications showed that SAM-PSO achieved the lowest overall cost, reduced travel distance by 82.1% and energy consumption by 66.5% relative to standard PSO, and converged 19.3% faster than ACO. These findings demonstrate the effectiveness of SAM-PSO for energy-aware multi-robot coordination in autonomous oil palm harvesting.

Keywords: multi-robot task allocation; energy-aware routing; memetic particle swarm optimisation; autonomous agricultural robotics; oil palm harvesting

P23: Adaptive Motion Planning and Obstacle Handling for Autonomous Oil Palm Harvesting

Alan Chung Shen Kai

Programme: MSc

Abstract

Autonomous oil-palm harvesting remains challenging due to dense canopy structures, where rigid obstacles coexist with compliant vegetation that obstructs access to fresh fruit bunches (FFBs). To address this issue, an integrated perception, motion-planning, and control framework was developed for a six-degree-of-freedom (6-DoF) robotic harvesting system. The framework combines red green blue-depth (RGB-D) sensing, Rapidly-Exploring Random Tree Connect (RRT-Connect) motion planning, and an adaptive obstacle-handling strategy to enable safe navigation and harvesting in cluttered plantation environments. Comparative evaluation of four motion planners demonstrated that RRT-Connect achieved the most consistent performance, with an average planning time of 0.021 s and stable trajectory generation. Field experiments showed that the proposed obstacle-handling strategy enabled a 60% harvesting success rate for occluded FFBs, while achieving 100% control success when the cutting point was correctly localized. These results demonstrate the potential of adaptive robotic harvesting for operation in unstructured oil-palm plantations.

Keywords: Oil-palm harvesting; autonomous robotics; motion planning; RRT-Connect; obstacle handling.

P24: Engineering Interparticle Gap in ZnO Nanorods for Enhanced SERS Performance: A Simulation-Guided Approach for Creatinine Detection

Izzah Hanaanah binti Ab. Aziz

Programme: PhD

Abstract

The interparticle gap between adjacent nanostructures plays a critical role in determining the electromagnetic enhancement and sensing performance of surface-enhanced Raman scattering (SERS) substrates. In this study, the influence of interparticle gap on the SERS performance of ZnO nanorods for creatinine detection was investigated through a combination of Finite-Difference Time-Domain (FDTD) simulation, field-emission scanning electron microscopy (FESEM), and Raman spectroscopy. FDTD simulations were performed using ZnO nanorod pairs with interparticle gaps of 40, 80, 120, and 160 nm to evaluate their electromagnetic enhancement behaviour. The simulation results revealed that the smallest interparticle gap of 40 nm generated the highest enhancement factor (EF) of 14.1 due to stronger electromagnetic confinement and hotspot formation. To experimentally validate the simulation findings, ZnO nanorods were synthesized at different temperatures (50, 80, 110, and 140°C) using a hydrothermal growth method. FESEM analysis showed that the sample synthesized at 80°C exhibited the smallest average interparticle gap of approximately 40 nm and the most compact nanorod arrangement. Consistent with the simulation prediction, SERS measurements demonstrated that the 80°C sample produced the highest creatinine signal intensity and experimental EF value of 30.00. The strong agreement between the FDTD simulation, FESEM characterization, and SERS measurements confirms that reduced interparticle gap enhances electromagnetic coupling and improves sensing performance. These findings demonstrate the effectiveness of simulation-guided optimization for designing high-performance ZnO nanorod-based SERS substrates and highlight their potential for sensitive creatinine detection and future biosensing applications.

Keywords: ZnO nanorods, Surface-enhanced Raman scattering (SERS), Interparticle gap, Finite-Difference Time-Domain (FDTD) simulation, Creatinine detection.

P25: Simulation-Based Capacitive Micromachined Ultrasonic Transducers Detection of Pulmonary Embolism

Hussnain Shahid

Programme: PhD

Abstract

Pulmonary embolism (PE) is a life-threatening cardiovascular condition that remains challenging to diagnose using existing techniques. This study investigates the feasibility of using a capacitive micromachined ultrasonic transducer (CMUT) for non-invasive PE detection through simulation. A thoracic acoustic model was developed in COMSOL Multiphysics to analyze ultrasonic wave propagation in healthy and embolus-affected lungs. The simulation results demonstrate measurable pressure variations caused by embolic obstructions, enabling the identification of suitable CMUT operating parameters. The findings support the potential of CMUT-based ultrasonic sensing for future non-invasive PE detection systems.

Keywords: Capacitive micromachined ultrasonic transducer (CMUT), pulmonary embolism, ultrasonic sensing, acoustic modeling, COMSOL Multiphysics.

P26: Performance Enhancement of Diketopyrrolopyrrole-dithienothiophene-Based Organic Thin Film Transistors (OTFTs) Using Solvent Variation

Reni Silvia Nasution[1], Norhayati Abu Bakar[1], Dee Chang Fu[1], Ahmad Ghadafi Ismail[1*]

[1]Institute of Microengineering and Nanoelectronics (IMEN), Universiti Kebangsaan Malaysia, 43600 Bangi, Selangor, Malaysia

*Corresponding email address: ghad@ukm.edu.my

Abstract—Organic semiconductors have emerged as promising materials for next-generation electronic devices owing to their inherent flexibility and compatibility with low-cost fabrication techniques. Diketopyrrolopyrrole-dithienothiophene (DPP-DTT) is a potential semiconductor material for OTFTs due to its high hole mobility, strong π–π interactions, and good stability. This study aims to observe the effect of solvent types (chloroform, chlorobenzene, and a mixture of chloroform-chlorobenzene) on the mobility of DPP-DTT-based OTFTs. DPP-DTT solutions were deposited using a spin coating method and the charge carrier mobility measurements were carried out. The results showed that the mixture of chloroform-chlorobenzene solvents produced higher mobilities up to 2.61×10^{-2} cm²/V.s and 4.86×10^{-2} cm²/V.s without treatment and with O_2 plasma treatment, respectively. The choice of solvent plays an important role in improving the performance of DPP-DTT-based OTFTs.

P27: Morphological and Strength Analysis of Lignocaine-Embedded Maltose-based Dissolvable Microneedles

Arifah Syahirah binti Abdul Rahman

Programme: PhD

Abstract

Microneedles is a minimally invasive transdermal drug delivery system that can address some limitations of conventional topical formulations and hypodermic needles. In this study, lignocaine-loaded maltose dissolving microneedle arrays were fabricated and evaluated based on formulation, morphology, and mechanical performance. Suitable formulation was established during mould filling process to ensure reproducible microneedle formation, before being observed under FESEM and tested for mechanical strength using texture analyzer (TA). Field-emission scanning electron microscopy showed that the fabricated microneedles had sharp tips and relatively uniform geometry. Mechanical testing using a texture analyzer was performed to assess whether the microneedles could withstand compression during application. Overall, the selected maltose–lignocaine formulation showed suitable processability, acceptable structural integrity, and adequate mechanical robustness. These findings suggest that maltose based dissolving microneedles have potential as a platform for minimally invasive local anesthetic delivery.

Keywords: dissolvable; microneedle; lignocaine; maltose; texture analyzer; scanning electron microscopy

P28: Optimization of Fabrication Parameters for Calcium Chloride-Maltose-Sodium Alginate Dissolvable Microneedles Based on Hardness Evaluation by Nanoindentation

Mohd Eusoff bin Azizul Nashriby

Programme: PhD

P29: Compact Dynamic Digital Frequency Divider Design for Low-Power Biomedical ADPLL Systems

Abdul Khaliq

Programme: PhD

Abstract

An efficient Digital Phase-Locked Loop (ADPLL) architecture is required for biomedical monitoring systems that depend on low-power frequency synthesis. However, frequency dividers are unsuitable for efficient biomedical applications due to high power consumption, increased phase noise, large area requirements, and integration problems. This research proposes a low-power, compact digital frequency divider for All-Digital Phase-Locked Loop (ADPLL) RF transceivers, aiming to enhance frequency-division accuracy while minimizing power consumption and hardware complexity for biomedical monitoring applications. The proposed digital frequency divider uses TSPC-based CMOS logic to overcome the limitations of conventional frequency dividers, including area, power dissipation, phase noise, and integration issues. This design dynamically switches between divide-by-2 and divide-by-3 modes, effectively achieving a divide-by-9 operation by using TSPC-based CMOS design, enhancing precise frequency scaling with low power consumption. Implemented using Verilog HDL and validated through simulation achieves stable operation with a divided output clock of 48.89MHz, derived from DCO output clock of 450 MHz and a 50 MHz reference frequency, ensuring smooth ADPLL integration for energy-efficient biomedical monitoring. The ability to scale and the design make it perfect for medical application driven by the Internet of Things and biomedical devices. The future research will be focused on the further optimization of power and the improvement of adaptability for advanced biomedical signal processing.

Keywords: Digital Frequency divider, ADPLL, RF transceiver, DCO, TSPC,

P30: Influence of Preparation Conditions on Phase Formation Hydrothermally Synthesized TiO2 Nanorods

Nahrusyifa' binti Abdul Karim

Programme: Phd

Abstract Titanium dioxide (TiO2) nanostructures were synthesized via a hydrothermal method under varying precursor conditions to determine how preparation parameters influence the final photocatalyst structure and performance. The objective of this study was to identify the dominant synthesis factors controlling anatase formation and to compare the structural differences between TiO2 prepared under acidic and alkaline conditions. The synthesized materials were evaluated using statistical analysis, X-ray diffraction (XRD), and Raman spectroscopy. Statistical analysis showed that pH was the dominant factor governing anatase formation, with a highly significant effect ($p < 0.001$), while processing time showed a trend but was not statistically significant. XRD analysis demonstrated that acidic conditions favored anatase formation and produced sharper diffraction peaks, indicating higher crystallinity compared with alkaline conditions. Raman spectroscopy further confirmed improved lattice ordering under acidic synthesis, as shown by stronger anatase Eg vibrational modes. Photocatalytic tests using methylene blue revealed higher degradation efficiency for TiO2 synthesized under acidic conditions, which was attributed to enhanced surface defects and surface area that promote reactive oxygen species generation. Overall, the findings show that precursor pH plays a critical role in controlling hydrolysis, condensation, anatase crystallization, and photocatalytic performance of hydrothermally synthesized TiO2 nanostructures.

Keywords; Titanium dioxide, hydrothermal synthesis, anatase, nanorods, photocatalysis

P31: Effect of Cu Substrate Surface Roughness on IMC Layer Growth Kinetics in Lead-Free Solder Joints

Muhamad Nur Syahiran bin Muhamad Yusof

Programme: MSc

Abstract

Abstract. The formation and growth of intermetallic compounds (IMCs) significantly influence the reliability of lead-free solder joints in electronic packaging. Excessive IMC growth during thermal aging can weaken the mechanical integrity of solder interconnections. This study investigates the effect of Cu substrate surface roughness on IMC layer growth in SAC305 solder joints under high temperature storage at 60°C. Different surface conditions were prepared using grinding papers with varying grit sizes ranging from P600 to P2000. The solder joints were aged from 250 h to 1000 h, and the IMC thickness was evaluated to determine the influence of surface morphology on interfacial reactions. The results showed that IMC thickness increased with aging duration for all samples due to continuous diffusion between Cu and Sn atoms. However, the IMC growth rate varied according to surface roughness. The P1000 surface condition exhibited relatively thinner IMC layers compared to the rougher P600 and smoother P2000 surfaces, indicating improved control of IMC growth. The findings suggest that optimized surface roughness can regulate diffusion kinetics and interfacial stability, providing a simple, environmentally friendly, and cost-effective approach to enhance solder joint reliability in advanced electronic packaging applications.

Keywords: Surface roughness, Intermetallic compound (IMC), SAC305 solder, Surface modification, High temperature storage

P32: The Effect of Silver Nanostars (AgNs) Layers as a SERS Substrate for Glucose Detection

Nur Ain binti Mohd Nasir

Programme: MSc

Abstract

The detection of glucose by using the Raman technique is a challenging problem because glucose molecules have a small Raman scattering cross-section and a low affinity for adsorption on metal

nanoparticle surfaces. Therefore, the SERS technique has been introduced to increase the Raman signal of glucose after absorbing the metal nanostructures' surface by simply tailoring the properties and surface chemistry of the nanostructures. It has been shown that SERS using silver substrates is a powerful tool for the identification and qualification of trace chemical analysis based on their unique molecular vibrations. SERS is a surface-sensitive technique that enhances the Raman signal of molecules absorbed on metal nanostructure surfaces and provides vibrational information for sample identification and quantitation. In this work, we report the synthesis of star-shaped nanostructures using silver as SERS-active elements to detect glucose. The SERS substrates were prepared with multiple depositions of the silver nanostars using a self-assembly approach to give a dense coverage of the AgNs on a glass surface, which ultimately increased the availability of the spikes needed for SERS activity. The SERS substrates developed in this work show very high sensitivity and excellent reproducibility. Hence, based on all of this, we attempt to observe the SERS performance for glucose detection.

Keywords: Glucose, SERS, silver nanostars (AgNs)

P33: Effect of UV Post-Curing on Heavy Metal Rejection Performance of 3D-Printed Composite Membranes

Noor Asnida Asli

Abstract

Three-dimensional printed graphene oxide based membranes offer highly tunable architectures for water treatment, yet the impact of ultraviolet (UV) post-curing on their functional performance remains insufficiently understood. This study investigates how UV post-curing time influences the heavy metal filtration and antibacterial efficacy of GO/acrylate composite membranes fabricated via Digital Light Processing (DLP). Fabricated membranes were post-cured under UV irradiation for 5, 10, 15, 20, and 25 min. Heavy metal filtrations specifically the rejection of cadmium (Cd), arsenic (As), and lead (Pb) was quantified using Inductively Coupled Plasma Optical Emission Spectroscopy (ICP-OES). Results revealed that Pb exhibited the highest filtration efficiency, peaking at 12.22% rejection after 5 min of UV post-curing, compared to a baseline of 7.66% at longer curing times. Conversely, Cd and As rejection remained below 3% across all conditions. These findings demonstrate that UV post-curing distinctively modulates the heavy metal filtration behavior of DLP-printed GO membranes, particularly for Pb. The study highlights critical baseline limitations and underscores the need for structural and compositional optimization to achieve viable heavy metal rejection in advanced wastewater treatment.

P34: Light-Driven Underwater Transport of Macroscale Soft Robots

Dhriti Neogi

Abstract

Optical tweezers for trapping and manipulating microscopic objects are limited by the strength exerted by electromagnetic forces. Strongly driven light–matter interactions in liquids offer a new technique for macroscopic optical actuation that is not limited by photon momentum. We introduce a new class of magneto-optofluidic photonic Curie engine that converts moderate continuous-wave photothermal energy into controllable torque and the translation of large objects at the air–water interface. The photonic Curie engine consists of a 3 cm hollow floating actuator containing a ferrofluidic core and a soot-blackened photothermal shell. Illumination with a 532 nm CW laser produces a localized temperature rise of approximately 10 C, which simultaneously lowers the local water surface tension and reduces the magnetic susceptibility of the ferrofluid. The reduced surface tension and the thermo-convective forces at the air-liquid interface provide a remotely controlled laser-driven linear momentum to a partially submerged floating object. In the presence of a vertical DC magnetic field, these coupled thermocapillary and

thermomagnetic gradients generate Kelvin-force-driven internal circulation of the ferrofluid. It leads to macroscopic rotation of the float and, by extension, of any object tethered to it.

The linear translation can be controlled by the incident laser power, whereas the torque imparted to the float can be controlled by the magnetic field strength and the thermal gradient in the presence of the laser field. The actuator exhibits reversible clockwise/counterclockwise rotation by repositioning the optical hot spot, with angular velocity increasing above a threshold near 0.3 W and reaching approximately 30° s^{-1} at 0.5 W. Control experiments using non-magnetic fills or transparent shells suppress the response, confirming that both photothermal absorption and ferrofluid magnetization are required. This light-powered platform enables contactless actuation of centimeter-scale soft robotic systems, including payload transport with carry-to-self weight ratios exceeding 1000, and establishes a scalable route toward fuel-free, programmable soft robots for surface and underwater applications.

Author Index

P

Q

R

S

V

W

X

Y

Z